Geomorphology 126 (2011) 297–313

Contents lists available at ScienceDirect

Geomorphology

journal homepage: www.elsevier.com/locate/geomorph

Field flume reveals aquatic vegetation's role in sediment and particulate phosphorus transport in a shallow aquatic ecosystem

Judson W. Harvey *, Gregory B. Noe, Laurel G. Larsen, Daniel J. Nowacki, Lauren E. McPhillips

U.S. Geological Survey, MS 430, 12201 Sunrise Valley Drive, National Research Program, Reston, VA 20192, Reston, VA 20192, USA

ARTICLE INFO

Article history:
Received 19 May 2009
Received in revised form 12 March 2010
Accepted 15 March 2010
Available online 7 April 2010

Keywords:
Hydroecology
Sediment transport
Floc
Wetland
Everglades
Phosphorus
Aquatic vegetation

ABSTRACT

Flow interactions with aquatic vegetation and effects on sediment transport and nutrient redistribution are uncertain in shallow aquatic ecosystems. Here we quantified sediment transport in the Everglades by progressively increasing flow velocity in a field flume constructed around undisturbed bed sediment and emergent macrophytes. Suspended sediment <100 μm was dominant in the lower range of laminar flow and was supplied by detachment from epiphyton. Sediment flux increased by a factor of four and coarse flocculent sediment >100 μm became dominant at higher velocity steps after a threshold shear stress for bed floc entrainment was exceeded. Shedding of vortices that had formed downstream of plant stems also occurred on that velocity step which promoted additional sediment detachment from epiphyton. Modeling determined that the potentially entrainable sediment reservoir, 46 g m^{-2}, was similar to the reservoir of epiphyton (66 g m^{-2}) but smaller than the reservoir of flocculent bed sediment (330 g m^{-2}). All suspended sediment was enriched in phosphorus (by approximately twenty times) compared with bulk sediment on the bed surface and on plant stems, indicating that the most easily entrainable sediment is also the most nutrient rich (and likely the most biologically active).

Published by Elsevier B.V.

1. Introduction

1.1. Physical–biological interactions in river and floodplain corridors

Feedbacks between hydrologic and ecologic processes are integral to the function of flowing aquatic ecosystems. Flood pulses deliver dissolved and particulate materials to surrounding floodplains that later slowly release particulate carbon, nutrients, and other energy-rich compounds back to the channel (Tockner et al., 2010; Noe and Hupp, 2009). Exchange between main channels and storage areas (e.g. slowly moving waters at channel margins and in streambed sediments) occurs under all flow conditions, and has similar effects in promoting storage and processing of solutes, fine sediments and associated carbon and nutrients (Newbold et al. 2005; Poole et al., 2008; Harvey et al. 2003). Redistribution of materials and energy between zones of fast moving flow and more slowly flowing areas further influences redox conditions and bacterial activity within sediments that affect metabolism and associated ecosystem functions (Odum et al., 1995; Middleton, 2002). Although coupling between channels, floodplains, and other storage areas is widely recognized (Junk et al., 1989; Bayley, 1991; Galat et al., 1998; Tockner et al., 2000), the transport processes are not necessarily well understood. In particular, there are many uncertainties about the transport of fine organic sediment and associated nutrients, and the role of vegetation in altering sediment transport. Yet the physical–biological interactions and resulting effects on sediment and nutrient redistribution are arguably some of the principal drivers of ecological function and hydrogeomorphic evolution of aquatic systems (Larsen et al., 2007; Bendix and Hupp, 2000; Tabacchi et al., 2000) and deserve more study. Attention is needed to understanding hydraulic, hydrogeomorphic, and biological controls on sediment and nutrient transport if the valuable functions of stream and river corridors are to be effectively preserved under increasing stresses of urbanization and climate change (National Research Council, 2002).

Compared with mineral particles, organic and organic–mineral sediment mixtures generally have lower densities and lower thresholds for entrainment from the sediment bed (Larsen et al., 2009a) and tend to be more varied in their sources and composition. Organic-rich sediment is typically composed of aggregates of detrital organic material and bacteria joined with varied types and sizes of mineral material (Lick et al., 1992; Sterling et al., 2005). Flocculation significantly influences fluxes and redistribution of sediment and associated nutrients or contaminants (Walling and Moorhead, 1989; Droppo, 2003, 2004). Predicting floc transport presents many challenges, as floccules vary widely in size, porosity, and density as determined by the type of organic matter, mineral sources and the nature of interparticle bonds (Logan and Wilkinson, 1990). Additional complexities include precipitation of minerals such as calcium carbonate which often occurs in periphyton mats and contributes to floc formation in hard water ecosystems (Browder et al., 1994) and

* Corresponding author. Tel.: +1 703 648 5876; fax: +1 703 648 5484.
E-mail address: jwharvey@usgs.gov (J.W. Harvey).

0169-555X/$ – see front matter. Published by Elsevier B.V.
doi:10.1016/j.geomorph.2010.03.028

also bacterial release of large quantities of extracellular polymeric substances that increase the strength of individual flocs (Simon et al., 2002; Battin et al., 2003; Wotton, 2007) and raise the bed shear stress needed to entrain floc (Gerbersdorf et al., 2008).

Emergent vegetation in shallow aquatic ecosystems plays a major role in determining flow velocity and turbulence characteristics that influence transport of flocculent sediment (Leonard and Luther, 1995; Leonard and Reed, 2002) and could also play a role as a source or sink for sediment (e.g. Elliott, 2000). Whether vegetation increases or decreases suspended sediment transport depends on how drag, near-bed turbulence, and entrainment are affected by flow interactions with stem diameter, density, and variability in the spatial arrangement and vertical changes in plant architecture (Nepf, 1999; Nezu and Onitsuka, 2001; Harvey et al., 2009). Most field investigations have observed that vegetation decreases suspended sediment concentrations (Braskerud, 2001; Leonard and Reed, 2002), either by increasing sediment deposition rates (Leonard and Reed, 2002; Leonard et al., 2006), or by direct trapping of sediment on stems and leaves (Saiers et al., 2003; Palmer et al., 2004; Huang et al., 2008). Vegetation also is suspected to serve as a source of suspended particles due to sloughing or hydraulically-driven detachment of fine sediment trapped by epiphyton on plant leaves, although direct observations of that process are scant.

1.2. Hydrogeomorphology of the Everglades, a low-gradient floodplain ecosystem

The Everglades is comprised of elongated, flow-parallel ridges and sloughs that formed several thousand years ago (Willard and Cronin, 2007; Bernhardt and Willard, 2009) (Fig. 1). The topographic and vegetation features are strikingly similar to other low-gradient, floodplain wetlands found worldwide that are valued for their relatively high biodiversity and high connectivity of habitats (e.g. Ellery et al., 2003; Stanturf and Schoenholtz, 1998). The past century has seen a rapid disappearance of the ridge and slough landscape pattern over large areas of the Everglades including flattening of the topography, greater homogeneity in vegetation, lower species diversity, and disruption of the connectivity of sloughs that otherwise provide migration corridors for aquatic organisms (National Research Council, 2003). Degradation of the Everglades ridge and slough ecosystem is in part attributable to altered water levels, though ridge-slough pattern loss has also occurred in areas where water levels have not changed substantially from historic conditions (National Research Council, 2003; Zweig and Kitchens, 2009). A leading hypothesis for ecosystem change is that the diminished peak flow velocities in the central Everglades that are presently on the order of 1 cm s^{-1} (compared with peak velocities approximately 6 times higher in the historic Everglades) are now insufficient to entrain floc and redistribute its associated carbon, nutrients, and mineral material from sloughs to the ridges (Larsen et al., 2007). The result in many areas is that ridge vegetation is expanding into the remnant sloughs, contributing to vegetative homogenization and topographic flattening over a significant proportion of the Everglades in just a century (Givnish et al., 2008), with a resulting loss of biodiversity and connectivity of Everglades habitats, two of the highly valued functional attributes of the Everglades.

This paper presents a flow experiment quantifying entrainment, size, and particulate phosphorus characteristics of naturally mobilized Everglades sediment as a function of flow velocity and bed shear stress (Fig. 1a). Our goal was to gain a better overall understanding of how flow affects organic sediment and phosphorus redistribution, a topic that is of crucial importance to Everglades restoration and more generally to streams and wetlands that are managed to optimize retention of suspended sediment and nutrients (Kadlec and Knight, 1996). We tested whether the higher flow velocities representative of the historic Everglades are sufficient to redistribute sediment and associated phosphorus from sloughs to ridges and thus contribute to long-term preservation of this topographically and biologically diverse landscape. Our study was needed because previous flume studies conducted in the Everglades either did not examine sediment transport (Gaiser et al., 2005), did not manipulate flow (Huang et al., 2008), used introduced "model" sediments that are not representative of the size and density characteristics of natural floc (Saiers et al., 2003), or, were conducted in laboratory flumes where the role of vegetation could not be examined (Larsen et al., 2009a, 2009c).

We increased flow in steps in a field flume and simultaneously measured floc mobilization, which allowed us to estimate the size of several important floc reservoirs (e.g. floc associated with epiphytic coatings on plant stems and floc on the bed surface) and to determine distinct hydraulic thresholds for entrainment from each of those reservoirs. Working in a field flume rather than a laboratory flume also had the advantage of minimizing disturbance that disrupts biofilms that strengthen floc. Our experiment allowed us to determine, possibly for the first time, the role of sediment resuspension from epiphyton and its contribution to downstream fluxes of suspended sediment and associated phosphorus. The results provide insight how future water management changes in the Everglades and elsewhere in other low-gradient aquatic ecosystems could affect redistribution of sediment and associated nutrients.

2. Materials and methods

2.1. Field site

The USGS experimental flumes are located in central Water Conservation Area 3A (26° 03′ 23.7″ N, 80° 42′ 19.2″ W) (Fig. 1). The Water Conservation Areas (WCAs) are large basins enclosed by levees that were constructed during the 1950s and 1960s for the dual purpose of managing water supply for the growing population of southeastern Florida while also allowing regulation of water flow to Everglades National Park farther to the south. The WCAs helped water managers ameliorate the excessive drying of the Everglades that occurred in the early and mid 1900s as a result of drainage and flood control measures. However, the WCAs also have drastically reduced flow velocities compared to pre-drainage conditions. Central WCA-3A was selected for the experiments because it has the best preserved area of the parallel-drainage ridge and slough landscape (Fig. 1a). These characteristic features consist of elongated sawgrass ridges (300–1000 m long by 60–160 m wide) interspersed with somewhat wider and less densely vegetated sloughs (140–360 m wide) in approximately a NNW–SSE alignment (Fig. 1b). Sloughs have a diverse assemblage of vegetation such as water lily (*Nymphaea odorata*), spikerush (*Eleocharis elongata*, with sparse *E. cellulosa*) with associated epiphyton, and floating bladderworts (*Utricularia purpurea*) and associated metaphyton (Fig. 1c). Ridges are typically 20–30 cm higher than intervening sloughs and are densely colonized by a nearly monospecific stand of sawgrass (*Cladium jamaicense*) (Fig. 1d). The ground surface in sloughs currently is approximately 20 cm lower than ridges with the transition from slough to ridge vegetation occurring over a 10–20 m horizontal distance.

The Everglades substrate is composed of organic peat formed by incomplete decomposition of plant material. On the surface of the peat is a layer of loosely consolidated floc that is dominantly organic matter (65% according to Bazante et al., 2006) and includes a range of floccule sizes (Larsen et al., 2009a) that are derived from various sources (Noe et al., 2007). Periphyton is a ubiquitous source of floc on submerged plant stems. It is composed of algal cells, macrophyte pieces, microbial cells, extracellular polymer substances, animal feces, and geochemical precipitates (principally calcium carbonate). When attached to stems and leaves of rooted aquatics, periphyton is referred to as epiphyton and when present in thick coatings on floating vegetation at the water surface it is referred to as metaphyton.

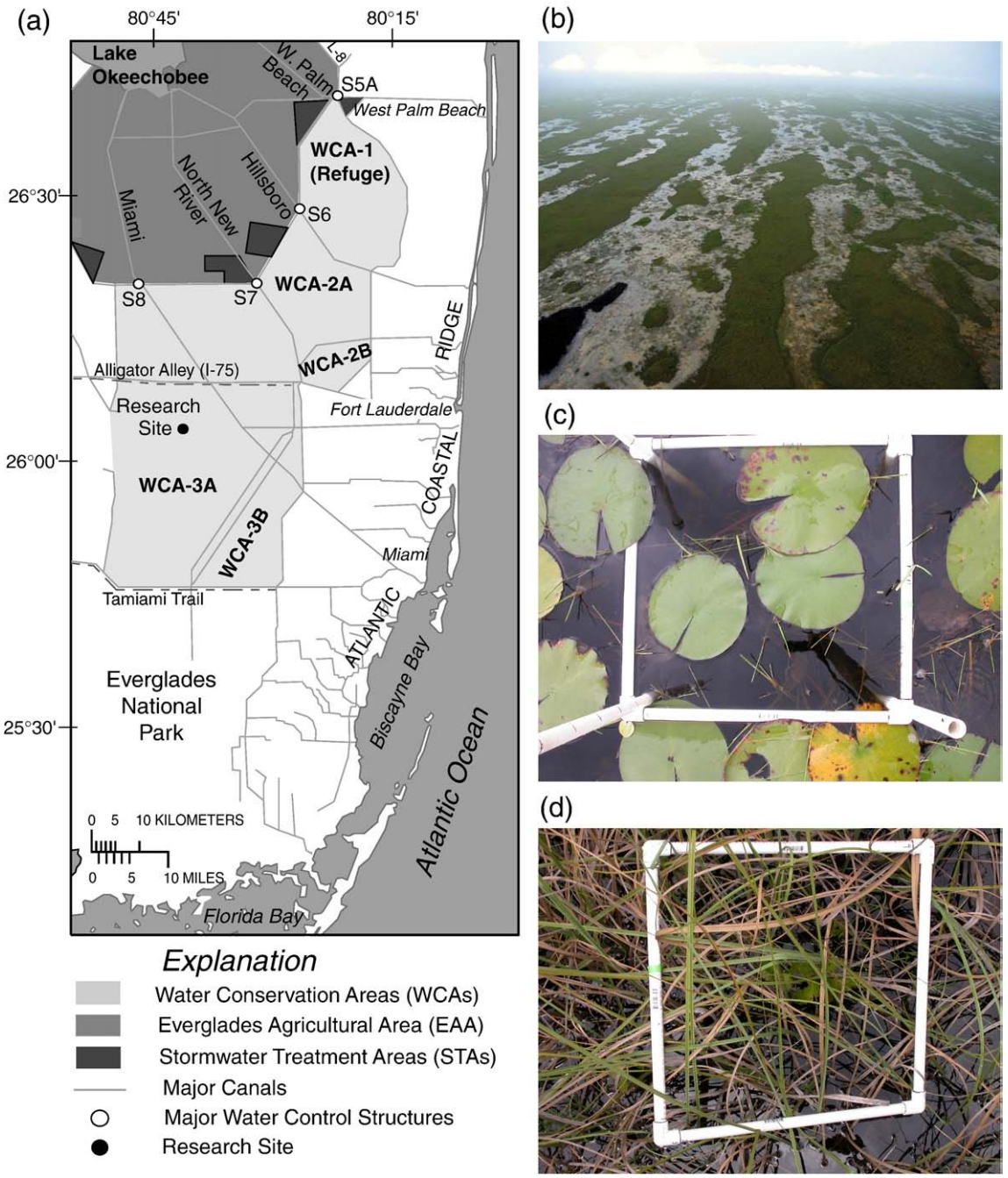

Fig. 1. The Everglades as it exists today with managed water conservation areas in light grey, areas converted to agriculture in medium grey, and the southern Everglades comprising Everglades National Park (a). Also shown are built features such as areas of constructed wetlands for removing excess nutrients (dark grey), and major canal–levee systems delineated by light grey lines. The site for field flume experiments is shown in an area of the central Everglades where historic ridge and slough landscape features are best preserved. Panel (b) is an oblique aerial photograph of the parallel-drainage ridge and slough features near the experimental flume site. The less densely vegetated sloughs are depicted as lighter areas and the slightly higher elevation and more densely vegetated ridges appear darker. Panels c and d provide a closer examination of slough and ridge vegetation communities as depicted by vertical overhead photographs taken approximately 2 m above the canopy (the sampling quadrant in each view is 0.5 m on a side).

Occasionally periphyton is present in a well defined mat on the sediment bed and is referred to as epipelon (Browder et al., 1994). More typically the sediment bed is composed of a relatively loose 3 to 7 cm thick layer of flocculent organic matter with periphyton components but without well developed epipelon mats. Beneath the bed floc is a layer of denser and more refractory peat (ranging between 0.6 m and 1.2 m thick in the central Everglades) that is situated above a sand and limestone aquifer system (Harvey and McCormick, 2009).

Wet seasons in the Everglades typically occur between May and October and alternate with dry seasons that typically last from November to April, depending on tropical storm and hurricane activity. Wet season precipitation, combined with regulation from control structures, keeps surface water depth typically in a range between 10 and 70 cm in sloughs. In the dry season water depths are typically shallower with some areas experiencing complete dry downs for weeks or months depending on climatic patterns and water releases from Lake Okeechobee.

The experimental site had the advantage of continuous measurements of flow velocity, water level, water temperature, air temperature, wind speed and direction, and precipitation between August 2005 and February 2008 (Harvey et al., 2009) and routine

measurements of suspended sediment characteristics (Noe et al., 2010). Our previous field flume experiments in the Everglades used introduced tracers (TiO_2 and fluorescent latex particles) to quantify dispersion characteristics and particle interception on vegetation stems (Saiers et al, 2003; Huang et al., 2008).

2.2. Field flume construction

Relatively small flumes are increasingly being used in field settings to manipulate flow speed in studies of sediment transport and aquatic ecology (e.g. Aberle et al., 2006; Gibbins et al., 2007). Less common are field flumes that are large enough that they can be installed around undisturbed bed sediment and naturally occurring aquatic vegetation. Our flume is 7.3 m long by 1 m wide constructed parallel to the ambient flow in an Everglades slough. The flume, its components, and the installed instrumentation are shown schematically in Fig. 2. The flume boundary walls were built using 0.2 cm thick PVC sheets inserted 0.1 m into the peat and held in place by external steel fence posts driven 0.75 m into the peat. This design protected the vegetation, peat, and flocculent organic sediment within the flume's interior from disturbance during construction. Both ends of the flume were left open, allowing flow through the flume at ambient speeds until just before the flow enhancement experiment began. A removable wall was attached at the downstream end of the flume prior to enhancing the flow under steady forcing created by three centrifugal pumps. The pumps were powered by a generator, which provided the capacity to withdraw surface water at a total rate of 0.67 m^3 min^{-1} from six fully-screened 2-inch (nominal) PVC wells located 0.3 m inside the closed end of the flume. The pumped water was exhausted downstream of the flume. Previous numerical simulations of this pumping configuration (Huang et al., 2008) confirmed that steady uniform flow was created throughout the majority of the flume with deviations toward radial flow into the wells only occurring within 0.5 m of the withdrawal wells.

2.3. Flow and suspended sediment measurements

Conditions for mobilizing organic sediment were determined in a flow enhancement experiment conducted on November 7, 2007 beginning at 12:00 P.M. Mean water column depth was 31.7 cm. The thickness of the flocculent sediment layer averaged 2.0 cm in the flume. During sequential flume runs at progressively higher velocities, the suspended sediment concentration was monitored by direct sampling of suspended sediment through peristaltic pumping of water from three surface water depths at each of three stations along a cross section of the flume. Methods are outlined in detail in Section 2.3.2. Concentration and size characteristics of suspended sediment were measured using two *in situ* sensors. The first sensor was a laser diffraction particle size analyzer (LISST-100X) that quantifies particles between the sizes of 1.25 and 250 μm. The second instrument was an underwater digital camera optimized to detect opaque particles larger than 43 μm. Details on the sensor measurements are given in Sections 2.3.3 and 2.3.4.

Before beginning flow enhancement we pumped water samples and initiated sensors. After 1 h of measurements during ambient flow (0.3 cm s^{-1}) the flume's downstream end wall was emplaced and sealed at its edges with waterproof packing tape. Three centrifugal pumps were immediately started to power the withdrawal wells at the flume's downstream end, followed by repetition of the suspended sediment monitoring. In total, flow speed was elevated in four steps (1.7, 3.2, 5.3, and 5.7 cm s^{-1}) with each step lasting approximately 1 h.

2.3.1. ADV monitoring of velocity profiles

Flow speeds and flume discharge at each velocity step are based on duplicate velocity profiles acquired using two 10-MHz ADVs (acoustic Doppler velocimeters; SonTek/YSI) deployed side by side to the left and right of the centerline of the flume at a distance of 4.4 m downstream from the flume start. Both ADVs measured velocities at nine vertical profile points in one-minute bursts. Vertical profiles of velocity were measured at least once and sometimes twice with each ADV during each flow enhancement step.

Velocity data were filtered and edited according to standard criteria suggested by the instrument manufacturer as well as specific criteria that were developed and refined in a prior Everglades study (Harvey et al., 2009). A minimum statistical correlation of 70% per sample and a minimum of 200 valid samples per burst were used as quantitative filters. Data with an acoustic signal-to-noise ratio (SNR) of 5 dB or less were subjected to additional quality assurance checks. The resolution of velocity measurements is 0.01 cm s^{-1}, with an accuracy of 1% of measured velocity. The resulting quality-assured measurements were time-averaged for each vertical increment and integrated vertically to compute a mean water column (i.e., depth-averaged) velocity at each step of flow enhancement (Fig. 3).

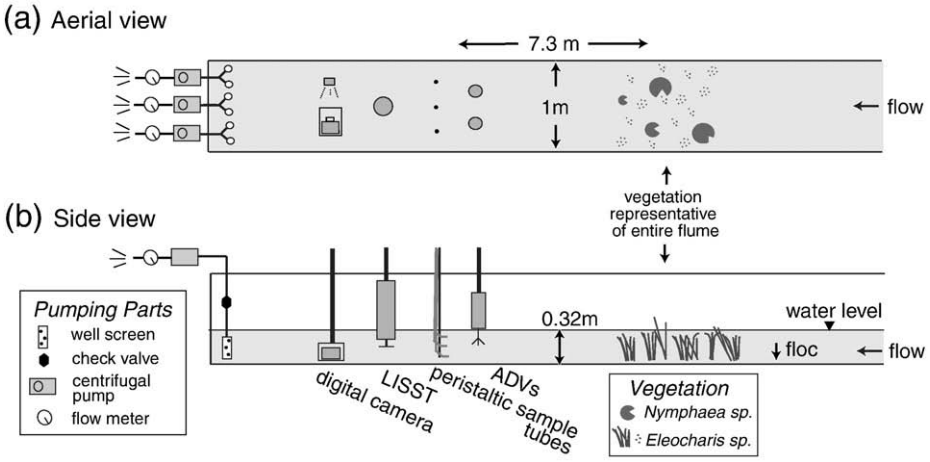

Fig. 2. Schematic of the field flume constructed on site in an Everglades slough. During periods when flow is not being increased by pumping the flume is open at both its upstream and downstream ends to allow ambient flow to pass through. Prior to flow enhancement a wall is emplaced at the downstream end, and flow is increased in steps from background ambient conditions (0.3 cm s^{-1}) up to approximately 6 cm s^{-1} using three centrifugal pumps. During the experiment flow velocity was measured by two ADVs, and suspended sediment concentration, size, and biogeochemical properties were determined by peristaltic pumping of samples and detection by laser diffraction imaging (LISST 100X), and by an underwater digital camera.

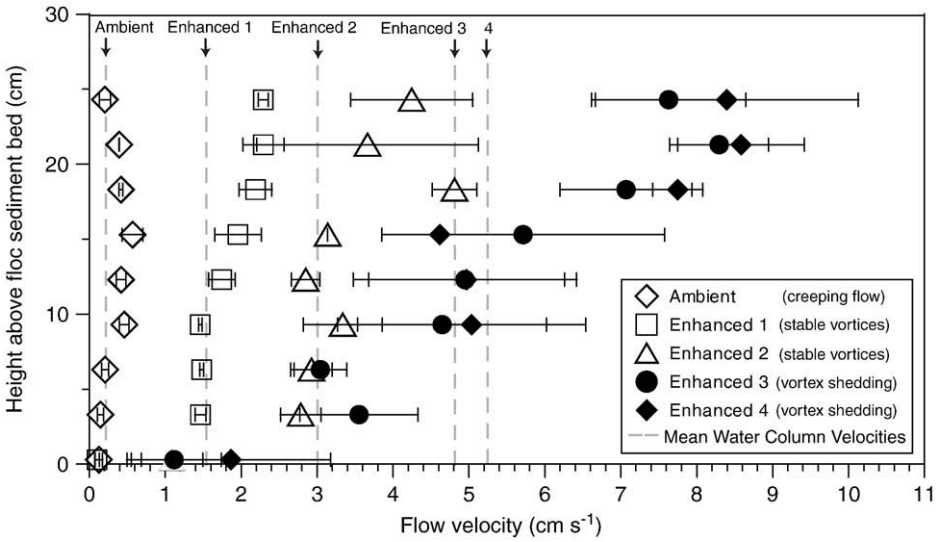

Fig. 3. Vertical profiles and depth-averaged flow velocities measured during ambient flow and four steps of flow enhancement in the field flume. Each step is characterized as being in a laminar regime characterized either by creeping flow (i.e. no vortices), stable vortices downstream of stems, or shedding on alternate sides of the vortices, based on the stem-based Reynolds number and on visual observations. Error bars plotted with the data points represent standard errors, obtained from duplicate profile measurements in time and space. Vertical dashed lines indicate the depth- and time-averaged values of velocity for each step.

Changes in bed shear stress during the flow experiment elucidate the likelihood of bed sediment entrainment. As bed shear stress increases beyond a critical threshold of entrainment, increasing amounts of flocculent sediment are entrained according to a power law relationship (Winterwerp and vanKesteren, 2004). For this experiment, bed shear stress was calculated using the measured vegetation characteristics and flow measurements for each experimental step. We used a flow model (Larsen et al., 2009b) that solves the governing equation for a one-dimensional steady, uniform force balance in which bed resistance and vegetative resistance balance the driving force (e.g. pumping at the downstream end of the flume), with water depth and water surface slope as independent variables. Vegetative resistance was predicted from the measured vertical velocity profiles, water depth, and measured stem architecture (Harvey et al., 2009) using a theory of momentum transfer in vegetation stem wakes (Nepf, 2004). Bed shear stresses were computed from the model profiles and compared to observations of sediment entrainment in the flume along with an empirical threshold bed shear stress for Everglades floc determined in a laboratory flume (Larsen et al., 2009a). The resulting bed shear stress estimates are considered accurate to within approximately ±20%. That uncertainty is based on numerical experiments in which bed shear stresses estimated from depth-averaged velocities were compared to those estimated from exact velocity profiles in *Eleocharis*-dominated slough communities (Larsen, 2008).

2.3.2. Direct measurements of suspended sediment by peristaltic pumping

Surface water was pumped from three depths in a cross section located 5.5 m downstream from the head of the flume. Duplicate peristaltic tubing lines (size 16 Masterflex) were fixed in place at "upper", "middle", and "lower" sampling depths (i.e., 8, 16, and 24 cm above the bed) at three positions (right-center, middle, and left-center) across the 1-m wide flume. At each sampling time water was pumped simultaneously from all levels and composited across the flume by depth at a combined pump rate of 840 mL/min. Two separate sample sets were collected at each sampling time (i.e. samples for sequential filtration (1 L) followed by samples for phosphorus extraction (300 mL)).

Sets of the two water samples were collected twice during each flow step, with the first collection beginning approximately 1 min after the three to five-minute period required to adjust the pumps and to allow flow through the flume to equilibrate at a new velocity. The second water sample was collected approximately 30–50 min later during each velocity step. Within 24 h, each sequential size filtration sample was sequentially filtered through 100 μm, 10 μm, 2.7 μm, 0.45 μm, and 0.2 μm filters by vacuum filtration. Each filter was then digested and analyzed for total phosphorus content (Noe et al., 2007). The mass concentration of suspended sediment in each size class was determined by drying and weighing each filter on a microbalance before and after filtration. The mass-weighted average sizes of particles were calculated using the mass concentration in each particle size class weighted by the geometric mean size of each of the five size class ranges (0.2–0.45 μm, 0.45–2.7 μm, 2.7–10 μm, 10–100 μm, and >100 μm). The geometric mean of the largest size class was determined using 1690 μm as the upper end of the size class, i.e. the size of the largest floc particle imaged in the analysis. The second water sample was filtered through only a 0.2 μm filter and then subjected to chemical extraction of microbial plus labile P. The phosphorus content and speciation into refractory sources, microbial sources, and other labile sources was determined using the methods of Noe et al. (2007).

Entrainment thresholds and characteristics of the sources of entrained sediment were examined by investigating trends in particle size and patterns of suspended sediment flux as a function of time and flow velocity. Suspended sediment flux was computed as the product of water flux and average sediment concentration at the time of each of the ten samples over the course of the experiment. Ten samples is a relatively sparse data set for temporal analysis but they constitute the primary data set for mass balance analysis because the alternative data sets from the LISST and underwater camera had relatively high uncertainty in the conversion from volume to mass concentrations, due to the large natural variability in floc density for a given floc diameter (see Larsen et al., 2009a). For that reason the pumped samples were the primary data set used to characterize the reservoir size of potentially mobilizable sediment and characteristics of source depletion as well as entrainment thresholds. Sensor data were used primarily to assess how aggregate size varied as a function of velocity, which provided additional information from which to interpret entrainment thresholds and source areas of sediment.

Sediment sources were frequently depleted during experiments where flow velocity was raised and we followed previous researchers

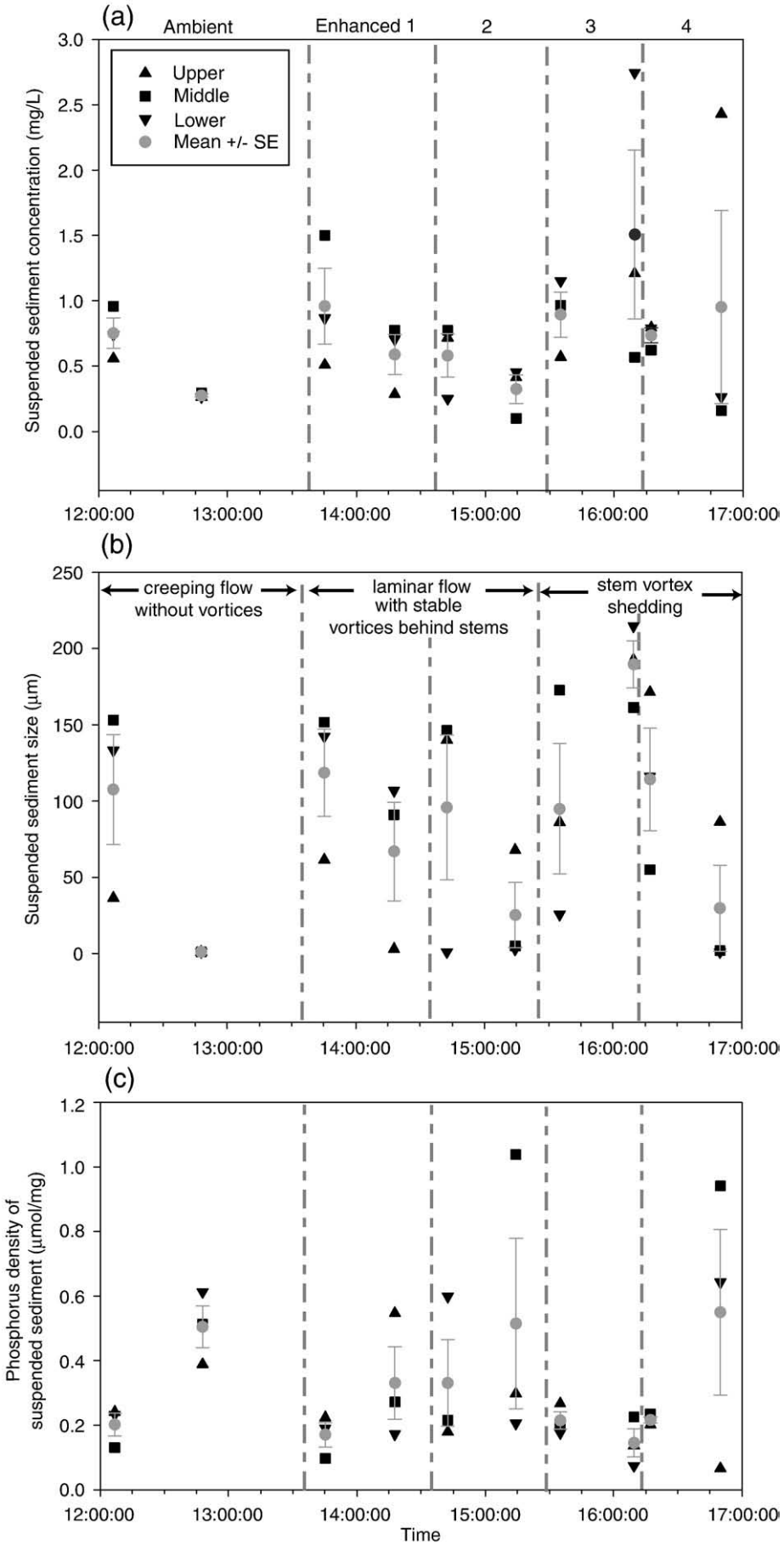

in expressing the decrease that occurs in the measured sediment fluxes using a simple impulse-response of the form:

$$J_e(t) = J_e(0)\cdot e^{-kt} \quad (1)$$

where J_e (t) is the entrainment flux of sediment in g m^{-2} d^{-1} measured after a given amount of time, t, has elapsed since the velocity was adjusted, J_e (0) is the initial entrainment flux measured momentarily after readjusting the velocity, and k is a rate constant with units of t^{-1} that is adjusted to fit the measured decrease in flux with time. The model for potentially entrainable sediment assumes first order dynamics of depletion, which is a typical observation in experiments of this type (Aberle et al., 2006). After a step change in velocity, the mean time before potentially entrainable sediment is mobilized is a sediment residence time that is equal to the inverse of the fitted rate constant, i.e. $T = 1/k$. In terms of measureable parameters, the residence time is equal to the size of the potentially entrainable sediment reservoir M, which has units of g m^{-2}, divided by the mean sediment flux during entrainment, J_e. The mean sediment flux is computed by calculating J_e after one residence time has elapsed, i.e. which is accomplished by using a value of k equal to 1 in Eq. (1). The size of the potentially entrainable sediment reservoir is estimated by rearranging the definition of residence time to compute M as $J_e \cdot T$. Calculated in this way, M estimates the total amount of sediment that would be entrained at a given velocity if velocity was held steady indefinitely rather than just for 1 h. In practice the calculation of potentially entrainable sediment at a given velocity needs to include the sediment that was actually entrained at the lower velocity steps that occurred earlier in the experiment. This definition assumes that the total potentially entrainable sediment reservoir at the current velocity step includes sediment entrained at lower velocity steps. The calculation of the total potentially entrainable sediment is therefore written as

$$M_n = \sum_{i=1}^{n-1}\sum_{j=1}^{m} J_e\cdot\Delta t + \overline{J}_e\cdot T_n \quad (2)$$

where M_n is the estimate of potentially entrainable sediment for the nth velocity step, Δt is the time increment used for calculations, i is a counter for the number of experimental steps, j is a counter for the number of time increments and m is the total number of time increments for a given flow step. Experimental flow steps 1 and 2 were analyzed separately. However, flow steps 3 and 4 were treated as a single flow step because the change in velocity from step 3 to step 4 (5.4 to 5.7 cm s^{-1}) was very minor.

Due to uncertainties in measured concentrations of suspended sediment, the magnitude of entrainment fluxes and the size of the potentially entrainable floc reservoir are also uncertain. Measured sediment concentrations especially varied with depth during the combined flow stages 3 and 4 (Fig. 4a). Two of the four measured concentrations during those flow steps had relatively high uncertainty. We chose to address uncertainty by modeling three scenarios of entrainment for flow steps 3 and 4 that represent the upper, middle, and lower bounds. The upper bound model used only the measurements with relatively large uncertainties for fitting while the lower bound model used only the measurements with smaller uncertainty. The middle bound model used all measurements and provided a prediction that falls between the upper and lower bounds. The three model scenarios differed, but with a relative uncertainty of approximately plus or minus 20% of the average of the estimates. Thus the uncertainty had relatively little effect on the interpretation of experimental results.

2.3.3. LISST-100X measurements of suspended sediment

In addition to directly measuring sediment transport we employed two methods of particle imaging. The first was a laser diffraction-based method and the second was a photo-imaging method described in the next section. The LISST-100X (Sequoia Scientific) measures diffraction of a laser beam by suspended sediment in water to estimate the volume concentration (in units of μL/L) as opposed to the more familiar mass-based concentration in μg/L. The LISST-100X also estimates the size distribution of suspended sediment *in situ* in 32 logarithmically-spaced `bins ranging in size between 1.25 to 250 μm. For our study the LISST was deployed vertically in the middle of the water column, with the top of the 5-cm long sample volume positioned at 16 cm below the water surface (i.e., at the midpoint of the water column) at the times that water sampling occurred. The LISST was programmed to collect ten bursts over 0.3 s that were averaged each second. Vertical profiling also was conducted during a two-minute period during the middle of each 1-hour velocity step. Unfortunately the vertical profiling caused minor fouling of the LISST-100X optics that required recalibration of the LISST between profile measurements. Fouling occurred due to settling of sediment on the optical window of the LISST as a result of disturbance and resuspension of fine particulates on plant leaves within the immediate vicinity. Since flow conditions were steady and suspended sediment concentrations were relatively steady during the short time period required for profiling, we recalibrated by differencing the measurements made before and after the profiling to account for the fouling.

2.3.4. Underwater digital camera imaging of suspended sediment

A digital single-lens reflex camera with a 60-mm macro lens (Nikon Corporation, Mellville, NY) was controlled remotely by a laptop computer to image larger suspended particles at a height of 8 cm above the bed. Using the equipment and procedures described by Larsen et al. (2009a), images were silhouetted by backlighting and binarized to provide maximum contrast between the floc and the background. The result was quantification of the concentration of suspended flocs down to a minimum diameter of 43.5 μm. Field comparisons with the LISST revealed that while the larger opaque particles could be resolved with this configuration, there was also a significant amount of material finer than the camera's minimum resolution, including translucent particles such as free-floating bacteria (Noe et al., 2007) that could not be resolved by photographic imaging. Conversion of underwater digital photographic imaging data from volume to mass units followed the same procedure used for conversion of LISST data (described in Section 2.3.5).

2.3.5. Estimation of floc particle densities

Volumetric concentrations of floc detected by the LISST and underwater camera required aggregate densities to convert to mass concentrations. A predictive relationship between aggregate size and aggregate density was developed from analysis of settling column data generated with bed floc collected from our research site (Larsen et al., 2009a). Aggregate dry density was determined for 20,280 particles up to 1690 μm in size (the largest particle detected). The analysis used Stoke's law and assumed that particles were spherical but with variable density over the range of particle sizes. Departures from sphericity could result in inaccurate estimation of particle density from settling columns, but from visual inspection under a

Fig. 4. Variation over time in suspended sediment concentration (a), mean size of suspended sediment aggregates (b), and phosphorus density of suspended sediment (c) measured by sequential filtration of pumped samples during steps of the enhanced flow experiment demarcated by vertical dashed lines. A pulse of sediment was entrained during enhanced flow steps 1 and 2 (characterized by laminar flow with stable vortices downstream of stems). By the end of enhanced flow step 2 there were indications that the source of entrained sediments was being depleted. A second larger pulse of entrainment is evident during enhanced flow steps 3 and 4 (characterized by a higher range of laminar flow when stem vortices were shedding). Error bars represent standard errors of the mean for the three depths of peristaltic pumping for each sampling time. Values for the individual depths are also shown.

microscope, we concluded that Everglades floc particles were better approximated as spheres than as rods or lamellae.

The practical lower boundary for determining dry aggregate density of floc in the settling experiment was 52 μm due to the camera's lower limit of detection of translucent aggregates. The densities of finer floccules were estimated from the settling column experiment based on independent information about the composition of Everglades floc. To estimate the aggregate densities of those finer flocs we used 1.3 g cm^{-3} for the wet density of detrital matter and bacteria (Cushing et al., 1993; Inoue et al., 2007), or 0.39 g cm^{-3} when expressed as a dry density (assuming that detrital macrophyte pieces and bacteria have a generally accepted water content value of 70%). A density of 2.71 g cm^{-3} was used for solid calcium carbonate, which was adjusted using a porosity of 65% to calculate a dry density of 0.95 g cm^{-3} for compound aggregates of $CaCO_3$. The porosity for $CaCO_3$ aggregates was estimated based on inspection of $CaCO_3$ primary particles in scanning electron microscope photographs made by other researchers (Kremer et al., 2008). After further adjustment to account for the average ratio of organic to mineral matter of 65% in Everglades floc (Bazante et al., 2006), the final estimate for the dry density for aggregates finer than 52 μm was computed to be 0.59 g cm^{-3}. Volumetric suspended sediment concentrations measured by the LISST and underwater digital camera were converted to mass concentrations by multiplying the volume concentration in each size class bin by the predicted dry aggregate density for that bin's average particle size (i.e. by using the power law relationship for bin sizes larger than 52 μm and 0.59 g cm^{-3} for smaller bin sizes).

2.4. Measurements of vegetation and depth of the flocculent sediment bed

Macrophytes within the flume were dominated by *N. odorata* and *Eleocharis elongata*, with sparse *E. cellulosa*, *Panicum hemitomon*, *U. purpurea*, and *Paspalidium geminatum*. The floating bladderwort *U. purpurea* was rare at our site at the time of the experiment. Macrophyte biomass and volume were measured in a 0.25 m^2 square clip plot adjacent to the flume that had similar vegetation to within the flume. Vegetation was clipped in 10-cm deep increments from the water surface to the peat layer, followed by sorting by species. When the plant samples were returned to the lab for this analysis, extreme care was exercised upon handling stems with epiphyton to reduce disturbance and compaction of the epiphyton. Diameter of stems with epiphyton present was measured in the middle of the stem at the widest dimension (major axis) using a micrometer, and then perpendicular to that (minor axis). After diameter was measured, the epiphyton was stripped from each stem using a Kimwipe. Stem diameter was then remeasured. Epiphyton mass was determined by drying samples at 60 °C to constant mass. Estimation of frontal area and stem diameter as they varied vertically in the water column followed Harvey et al. (2009) with the addition of a second set of calculations to quantify the contribution of epiphyton.

The depth and bulk density of flocculent sediment on the bed was measured outside the flume and also inside the flume after the experiment was concluded. Floc samples were taken at five equally spaced locations along the flume axis. A vertical core through the water column and floc into the peat was taken with a 2-cm inner diameter clear acrylic tube. The top of the floc layer was marked on the tube, a circular sponge affixed to the end of a dowel was lowered through the water in the tube to the marked interface, and surface water was poured off through the sponge. Floc was then sampled by pouring it out of the tube into a sample container. The top of the peat was then marked on the tube. Floc depth was determined as the distance between marks on the tube that identified the top of the floc and the top of the peat. Bulk density of each floc sample was determined by drying samples at 60 °C to constant mass, weighing the dry sample, and dividing by the area of the corer multiplied by floc depth.

3. Results

3.1. Flow hydraulics in the field flume

The flow enhancement experiment increased the flow from the ambient velocity of 0.3 cm s^{-1} to 5.7 cm s^{-1} in four steps. Based on measured depth-averaged velocities and vegetation stem diameters, the flow regime was characterized by a stem diameter-based Reynolds number, Re_d. The ambient hydraulic condition in the flume, typical of the Everglades (Harvey et al., 2009) was characterized by a relatively low value of 3 for Re_d which is in a range that is referred to as creeping flow because of the lack of formation of flow vortices downstream of stems (Sumer and Fredsoe, 2006). Flow remained laminar during the first and second enhanced flow steps (1.7 and 3.2 cm s^{-1}, Re_d values of 19 and 35, respectively) although the flow regime had changed with incipient vortices forming behind stems during those velocity steps. Flow also remained laminar during enhanced flow steps 3 and 4 (velocities of 5.3 and 5.7 cm s^{-1}, Re_d values of 58 and 63, respectively), however the vortices had begun shedding from alternating sides of the stems (i.e., a von Karman vortex street). Initiation of vortex shedding was not only evident visually but was also evident from the increase in variability of the measured flow velocities during flow steps 3 and 4 (Fig. 3). According to Nepf (1999) and references cited therein, stem vortex shedding begins to occur at Re_d greater than 40–50, which was consistent with our observations. Progression from a transitional to fully turbulent wake is expected to occur at a Re_d of approximately 200, which was not reached in our experiment.

Bed shear stress in the flume increased with each step of flow enhancement, beginning with an increase from 0.0008 to 0.004 Pa between ambient flow and enhanced flow step 1 followed by an increase to 0.008 for enhanced flow step 2. According to the results of laboratory flume experiments with Everglades floc (Larsen et al., 2009a), bed sediment should not have been entrained until approximately 0.01 Pa, which in our experiment was exceeded during enhanced flow step 3 (bed shear of 0.019 Pa) and was coincident with onset of stem vortex shedding. The final experimental velocity step (enhanced step 4) only increased velocity and bed shear stress (0.022 Pa) slightly.

3.2. Trends in concentration and size of entrained floc

The directly measured concentration of suspended sediment in pumped water samples was very low (0.51 mg L^{-1}) under ambient flow conditions. The suspended sediment concentration increased modestly to an average of 0.61 mg/L when velocity was increased by approximately an order of magnitude to values still within the laminar flow range during enhanced flow steps 1 and 2. The concentration of suspended sediment increased more substantially to an average of 1.02 mg/L during enhanced flow steps 3 and 4, as velocity was increased high enough to create flow conditions characterized by von Karman vortex shedding from stems. At ambient flow the average size of floc was 54 μm, which increased to an average of 77 μm during the first two increased velocity steps, characterized by laminar flow. After flow was increased enough to create vortex shedding conditions, the average diameter of floc increased to 107 μm (Table 1). Average floccule size tended to always increase at the beginning of new flow steps and then decrease until the time of the next flow step. Depth trends in suspended floc concentration and size are not as readily apparent as temporal trends (Fig. 4).

The highest suspended sediment concentration (2.5 mg/L) and the largest average floc diameter (210 μm) measured in pumped water samples were collected closest to the flocculent sediment bed during

Table 1
Summary of Flow and Suspended Sediment Transport During a Flow Enhancement Experiment on November 7, 2007 at Everglades Site 3A-5 in the "Slough" Flume. Flow was laminar during all experimental velocity steps according to the criteria Redb200. Flow interactions with stems ranged from creeping flow for ambient conditions to stable, wake-like vortices downstream of stems during enhanced flow steps 1 and 2, to repeated shedding of vortices from alternate sides of stems during enhanced flow steps 3 and 4. Sediment characteristics are based only on peristaltic-pumped samples.

Experiment stage	Flow interaction with vegetation stems	Velocity ($cm\ s^{-1}$)	Stem Reynolds number (Re_d)	Bed shear stress[a] ($Pa) \times 10^{-2}$	Estimated entrainable sediment ($g\ m^{-2}$)	Suspended sediment concentration (mg/L)	Average particle size (μm)	Particulate phosphorus (μM)	Particulate phosphorus density (μmol/mg)	% Microbial particulate phosphorus	Suspended sediment flux (mg/s)	Particulate phosphorus flux (μmol/s)
Ambient flow	Creeping flow	0.3	3	0.08		0.51	54	0.14	0.35	58	0.3	0.1
Enhanced 1	Stable Vortices	1.7	19	0.4	4							
Enhanced 2	Stable vortices	3.2	36	0.8	6	0.61+	77	0.14	0.34	56	4.1	1.0
Enhanced 3	Vortex Shedding	5.3	58	1.9	46							
Enhanced 4	Vortex shedding	5.7	63	2.2		1.02*	107	0.17	0.28	56	14.1	2.3

+ — sediment characteristics in this row are averages for enhanced flow steps 1 and 2.
* — sediment characteristics in this row are averages for enhanced flow steps 3 and 4.
[a] 1×10^{-2} Pa is a previous estimate of the critical shear stress for entrainment of bed floc in the Everglades made in a laboratory flume (Larsen et al., 2009a).

the latter part of flow step 3, after stem vortex shedding began. Consistent with that observation, the underwater camera, deployed only 8 cm above the bed, recorded the largest average size of floc during flow steps 3 (750 μm) and 4 (760 μm). This doubling of size at step 3 contrasted sharply with the minor variation in floc size that occurred during lower velocities (310 μm during ambient flow, 480 μm during velocity step 1, and 360 μm during velocity step 2). Concurrent with the change in hydraulic condition on flow step 3, the bed shear increased from 0.008 to 0.019 Pa (Table 1), which indicates that the threshold bed shear stress for Everglades' floc entrainment (0.01 Pa) estimated by Larsen et al. (2009a) was exceeded at the onset of vortex shedding flow conditions.

3.3. Trends in aggregate density of transported flocs

Coincident with increases in the suspended floc concentration and average size of floc at higher velocities, the average density of floc decreased. Fig. 5 shows the relationship between floc aggregate density and floc size that we determined from results of a settling column experiment using bed floc collected in the Everglades (Larsen et al., 2009a). Dry aggregate density of Everglades floc is shown in Fig. 5 to be a strong negative function of aggregate size:

$$\rho_{dry} = 1.19 \times 10^3 \cdot d^{-1.92} \quad (3)$$

where ρ_{dry} is the dry aggregate density of floc in $g\ cm^{-3}$ for particles ≥ 52 μm and d is floc diameter in μm. Smaller flocs were below the limit of detection of the digital camera for the settling experiment and were independently estimated to have a density of $0.59\ g\ cm^{-3}$ (see Section 2.3.5).

Everglades floccules are composed of aggregated particles that vary widely in size. Densities of the larger suspended floccules are relatively low, indicating the tendency of larger flocs to possess higher inter-aggregate porosities (Larsen et al., 2009a). A smaller contribution from mineral precipitates may also contribute to the smaller densities of larger floccules (Noe et al., 2007). The settling column data (Fig. 5) make clear that the more variable and generally higher densities of smaller floccules derive in part from a greater contribution from relatively dense mineral particles derived from precipitation of $CaCO_3$ in periphyton. A mineral source is evident from densities of individual aggregates as high as $2.7\ g\ cm^{-3}$ (which can only be the result of mineral inputs) as well as from Bazante et al.'s (2006) estimate of the contribution from mineral matter (35%). Precipitation of $CaCO_3$ is the most likely mineral source given the general lack of suspended silt and clay in Everglades source waters (Noe et al., 2007) as well as frequent observations that surface waters in many parts of the Everglades are often near saturation with respect to $CaCO_3$, and finally from widespread observations of $CaCO_3$ precipitation in periphyton in the Everglades as a result of pH adjustments in the metabolizing periphyton (Browder et al., 1994).

Changes in average density and size of suspended floc during each stage of the flow enhancement experiment are also shown in Fig. 5. For both the pumped water samples and the sensors, the average floc diameter increased and the density decreased sharply in the transition from ambient flow conditions to enhanced flow. From a transport perspective, these data make clear that larger flocs contribute more to an increase in the volume of mobilized sediment than they do to an increase in the mass of mobilized sediment. As experimental velocities were stepped up there were further increases in size of aggregates and decreases in aggregate density, but these changes were relatively small compared to adjustments that occurred in size and density of suspended floc on the initial step of flow enhancement (Fig. 5).

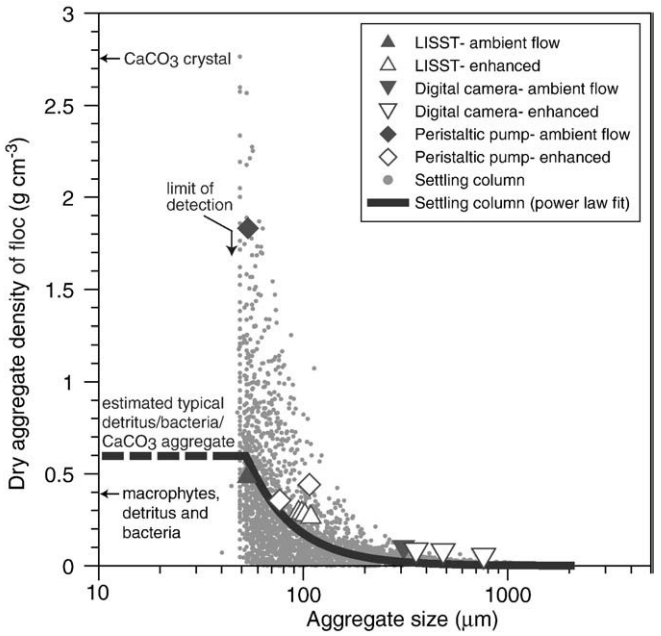

Fig. 5. Aggregate dry density (dry weight/wet volume) determined by collection of floc from an undisturbed area of the slough near the field flume for use in a laboratory settling experiment (Larsen et al. 2009a). Density is a strong negative function of particle size that was best described by a power law for particles between 52 μm (the limit of detection for the camera) and 1700 μm (the largest particle detected). Below the camera's detection limit the average density of small particles was estimated to be 0.59 g cm^{-3} (see text). A labeled arrow points to the dry density of calcium carbonate, which suggests that the upper bound for density of Everglades floc is established by primary particles of $CaCO_3$. The "macrophyte detritus and bacteria" arrow points to a typical density for primary particles of those organic materials. Note that many of the observed aggregates had lower densities, which is consistent with the expectation that floc is composed of porous aggregates with a lower overall density than the primary particles. Also plotted are estimates of the mean density of suspended aggregates detected during flow enhancement by peristaltic pumping (diamonds), laser diffraction (triangles), and the underwater camera (upside down triangles) which all show increasing size and decreasing densities of suspended aggregates under flow enhancement. The densities of aggregates collected by peristaltic pumping were determined directly by sequential size filtration and gravimetric methods, whereas densities for laser diffraction and underwater camera measurements (which only detect sediment volume) had to be converted to mass-based estimates using the gravimetric results from the pumped samples.

3.4. Temporal trends in floc entrainment during enhanced flow

Fig. 6 shows how the suspended sediment flux varied over time and with changing velocity. Fluxes are scaled on a per unit area basis relative to the contributing area of the bed inside the flume. An initial observation about the results in Fig. 6 is the indication that entrainment of floc occurred on all velocity steps. Within each experimental velocity step, sediment entrainment exhibited a pulse-like behavior with peak entrainment occurring very soon after velocity was increased followed by a relaxation in the rate of sediment entrainment until velocity was experimentally increased again. After each step increase in velocity, entrainment was again boosted as sediment from new and more resistive sources was mobilized. For example, entrainment was observed during enhanced flow step 1 followed by a relaxation in the entrainment flux until next velocity step. The cycle was repeated at the enhanced flow step 2 although the peak flux was lower (Fig. 6), suggesting that there was a depletion of sediment sources that could potentially be mobilized under laminar flow conditions with stable stem vortices. After flow had increased enough that stem vortices began shedding (on enhanced flow step 3) the entrainment flux increased markedly, indicating a new and significant source of sediment was being mobilized under the stem vortex shedding regime (Fig. 6).

Consistent with source depletion in the early stages of flow enhancement, mean particle size initially increased near the beginning of each flow step but generally declined through the first two velocity flow steps, indicating that the coarser flocs that could potentially be mobilized were mobilized early and then became scarcer. In particular, during the first enhanced flow step, the mean size of entrained floc was initially 120 μm but declined to 65 μm by the end. Then, following the increase to the second enhanced velocity, floc size increased to a lower peak value of approximately 100 μm and then declined to 34 μm by the end of that flow step (Fig. 4b). After flow vortex shedding from stems began on flow steps 3 and 4, floc size generally increased (up to 200 μm) but was back below 50 μm two hours later after easily entrainable floc sources had been depleted.

3.5. Potentially entrainable reservoirs of floc

The sizes of potentially entrainable floc reservoirs were estimated based on modeling temporal changes in sediment entrainment (Fig. 6 and Table 1). Laminar flows unexpectedly mobilized floc under conditions below a laboratory-determined threshold for floc entrainment from the bed. Sediment entrainment under those conditions was relatively small however (total size of 8 g m^{-2}). After stem vortex shedding began, the rate of cumulative entrainment increased markedly (Fig. 6) and revealed a potentially entrainable floc reservoir under vortex shedding conditions that was five times greater than what it was during laminar flow with stable vortices (i.e. 40–60 compared with 8 g m^{-2}) (Table 1). When compared with independent measurements of sediment reservoirs on the flocculent bed and as epiphytic coatings on plant leaves (Table 2), the potentially entrainable reservoir of floc is similar to epiphyton (66 g m^{-2}) but smaller than the reservoir stored on the bed in an approximately 2-cm deep layer of flocculent sediment (330 g m^{-2}). We observed that the total amount of floc that was present on the sediment bed was not greatly depleted by flow enhancement (Table 2), suggesting that not all Everglades bed floc is potentially entrainable at flow velocities less than 6 cm s^{-1}.

3.6. Patterns of phosphorus mobilization and transport with suspended floc

Unlike suspended floc concentration and average size of flocs, which increased at higher flow velocities, the concentration of sediment-associated phosphorus in water held fairly steady at approximately 0.14 μM as flow was increased from the ambient velocity to higher laminar flows during enhanced flow steps 1 and 2. The phosphorus concentration only increased slightly (0.17 μM) after stem vortex shedding began (Table 1). Although the concentration of sediment-associated phosphorus changed by a minor amount as flow velocities changed (Table 1), the phosphorus density in the floc (μmol/mg) varied by more than a factor of 3, ranging between values of 0.16 and 0.55 μmol/mg (Fig. 4c). Higher phosphorus density in smaller flocs indicates that relatively small flocs tend to be more enriched in phosphorous, containing a greater amount of phosphorus per unit mass of floc mass compared with larger flocs. To avoid confusion it is worth noting that the greater inter-aggregate porosity of larger flocs is not a factor in explaining the negative relationship between phosphorus density and size of flocs because the effect of porosity is controlled for in the calculation of phosphorus density.

Fig. 4b and c suggests that the phosphorus content of suspended particles is a function of the size of suspended flocs. Because the overall tendency was for the size of suspended flocs to increase at higher velocities, there was generally a corresponding decrease in phosphorus density of floc at higher flows. However there was considerable variation within each velocity step in floc size and its phosphorus density, indicating that biogeochemical characteristics of suspended sediment do not always exhibit simple relationships with

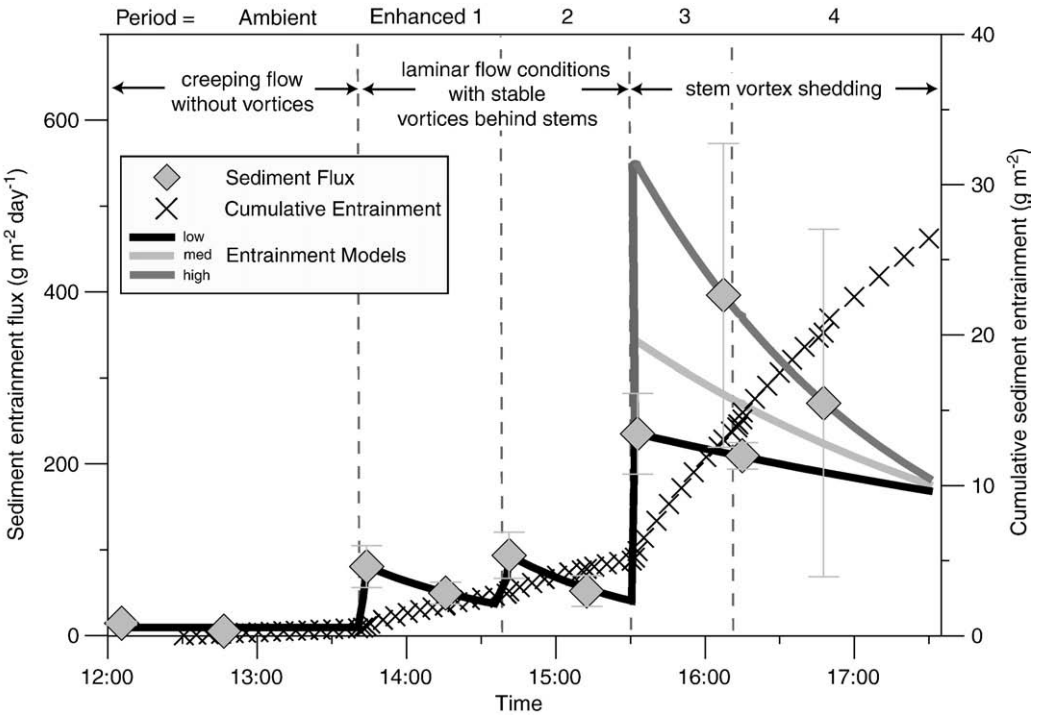

Fig. 6. Sediment entrainment fluxes, cumulative entrainment, and models used to estimate potentially entrainable sediment reservoirs. Entrainment was initially small under creeping and stable vortex flow conditions and then increased with the change to vortex shedding conditions characterized by von Karman vortex shedding from plant stems. Three scenarios were modeled for entrainment under stem vortex shedding conditions. The "high" and "medium" entrainment models decrease more quickly in their fluxes and produce similar estimates of potentially entrainable sediment (45 and 46 g m^{-2}) compared with the "low" entrainment model, which estimates more potentially entrainable sediment (69 g m^{-2}) due to an entrainment flux that decreases more slowly over time. Because the "medium" entrainment model matched the "high" model and was conservative toward not overestimating potentially entrainable sediment, it was selected as the best estimate to summarize the experimental results.

flow. During each step the larger and more phosphorus-poor floc tended to be entrained first followed by entrainment of smaller floc with higher phosphorus density (Fig. 4c), suggesting that after a sudden increase in velocity, the larger and more phosphorus poor component of the suspended floc becomes depleted and is replaced by entrainment of smaller and more enriched floc. Eventually the overall supply of large and small flocs that is potentially entrainable at a given velocity step is depleted. The cycle then repeats at the next highest flow step. Even after considerable entrainment had taken place in our experimental flume and stem vortex shedding was initiated, there still remained a supply of relatively small, phosphorus-enriched floccules to be entrained at the next highest velocity step.

Enhancement of flow velocity had the effect of increasing both the overall suspended sediment flux through the flume as well as the flux of sediment-associated phosphorus (Table 1). However, the approximately 70 times increase in suspended sediment flux at the highest flow was undercompensated by only a 25 times increase in phosphorus flux. The reason for the lower proportional increase in phosphorus flux was the tendency for suspended sediment to become coarser and less phosphorus-rich over extended time periods of elevated flow (Fig. 4c). Under-compensation in the growth of the particulate phosphorus flux during the experiment relative to the suspended sediment flux was especially pronounced at the highest two flow steps when entrainment of the coarser bed sediment was occurring (Table 1 and Fig. 4c).

3.7. Characteristics of suspended floc determined by the LISST and underwater camera

Like the pumped water samples, the LISST-100X detected a relatively large increase in suspended sediment concentration after switching from ambient flow to enhanced flow step 1 (0.23 mg/L to 1.22 mg/L), then a smaller increase to 1.30 mg/L during enhanced flow 2 (Fig. 7). The mean mass-weighted diameter of particles

Table 2
Characteristics of sediment reservoirs during a flow enhancement experiment on November 7, 2007 at Everglades site 3A-5 in the "slough" flume.

Flocculent bed sediment (pre- and post experiment)	Bed floc reservoir size (g m^{-2})	Bed floc depth (cm)	Bed floc bulk density (g cm^{-3}) $\times 10^{-2}$
Pre-experiment	330 ± 170	2.0 ± 0.4	1.51 ± 0.8
Post experiment	310 ± 180	2.0 ± 0.3	1.14 ± 0.4
Epiphyton on macrophytes (pre-experiment only)			**Epiphyton reservoir size (g m^{-2})**
All macrophytes			66
Eleocharis elongata			48
Eleocharis cellulosa			7
Paspalidium germinatum			6
Nymphaea odorata			5

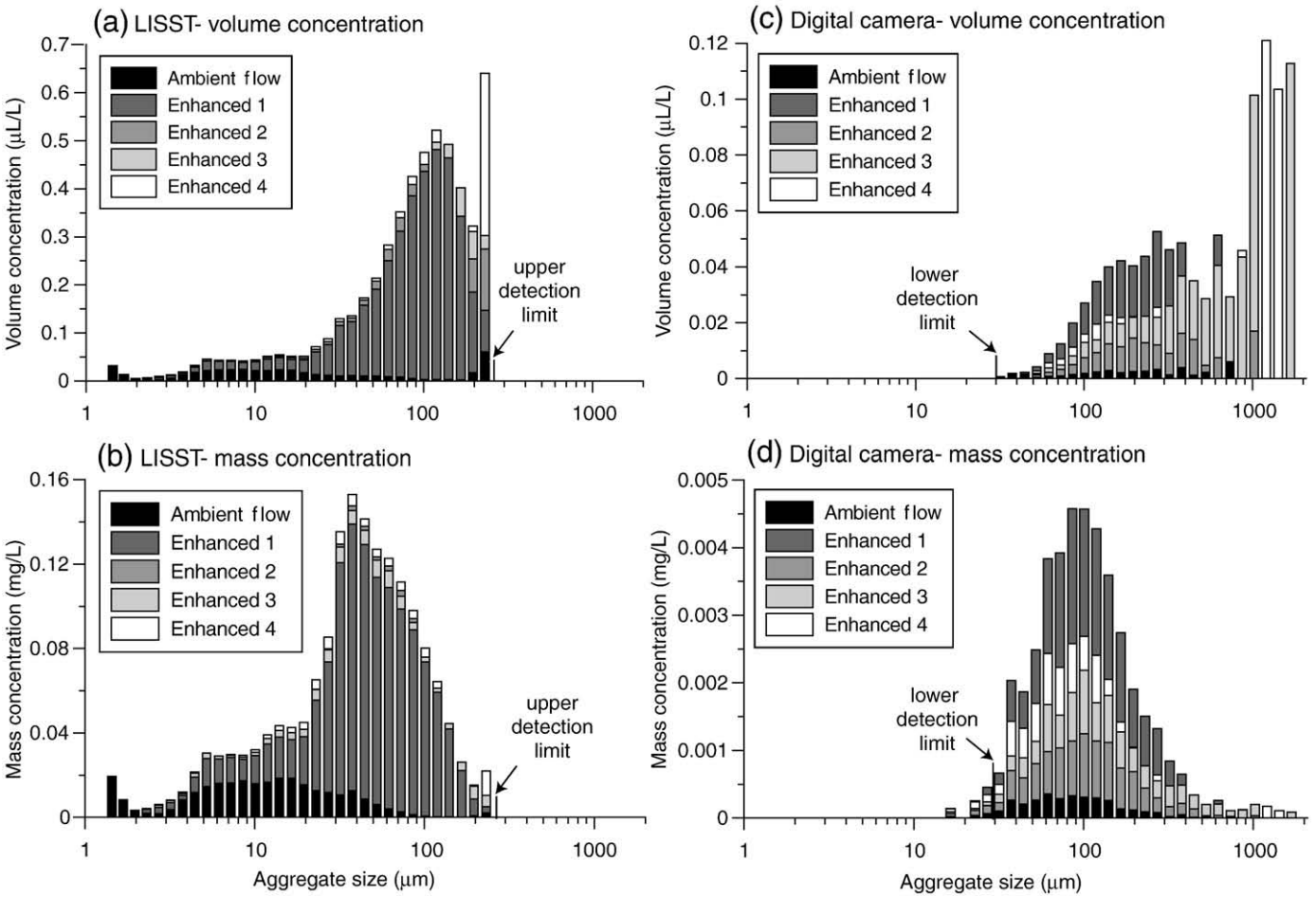

Fig. 7. Volumetric and mass-based concentrations of suspended sediment detected by laser diffraction (a and b) and by underwater digital camera (c and d) plotted versus aggregate size for each step of flow enhancement. Note the lower and higher size ranges, respectively, for detection of aggregates using laser diffraction and the digital camera.

increased from 18 μm at ambient flow to 56 μm during enhanced flow step 1 and then remained relatively steady at 56 μm during enhanced flow step 2. Further increases in suspended sediment concentration detected by the LISST (up to 1.4 mg/L during enhanced flow step 4) were minor.

The underwater digital camera also detected an initial pulse of suspended sediment after switching from ambient flow to enhanced flow step 1. However, due to the limitations of imaging small or translucent floccules, the suspended sediment concentrations were considerably lower than indicated by the LISST or by pumping samples. At ambient flow the concentration detected by the camera was 3×10^{-3} mg/L, which increased by an order of magnitude to 4×10^{-2} mg/L during enhanced flow step 1 followed by a reduction at the next step (to 1×10^{-2} mg/L) (Fig. 7d). The mean volume-weighted diameter of floc detected by the camera was 309 μm at ambient flow but increased to 482 μm at enhanced flow 1 and then back down to 356 μm during step 2. A second major entrainment pulse occurred during enhanced flow step 3, when concentration increased to 2×10^{-2} mg/L and floc size increased to 752 μm, and then suspended concentrations and floc size held relatively steady at 2×10^{-2} mg/L and 762 μm respectively during enhanced flow step 4.

One reason for substantial differences in detection of mass concentrations by the sensors is that the digital underwater camera and LISST detected flocs in different size ranges. Whereas the LISST detected floc of a size similar to what was detected by sequential filtration of pumped water samples, the underwater camera detected larger aggregates due to a higher range of detection of aggregate sizes compared with the LISST. The underwater camera was also better able to detect large flocs than sequential filtration of pumped samples, which may have disaggregated floccules during pumping. Comparison of panels b and d in Fig. 7 indicates that the large particles detected by the camera were typically 30 times lower in their mass concentration than the LISST values due to the inherent limitations of the camera imaging of smaller, denser, and more translucent flocs. Despite the lower estimates of mass concentrations, the camera was useful in revealing patterns in the entrained floc. For example, the underwater digital camera, which was positioned low in the water column relative to the LISST and which could detect larger particles, observed a doubling of mean size of entrained flocs as flow changed in character from stable vortices behind stems to a vortex shedding regime. The underwater camera supplied the most direct evidence that significant bed sediment was only entrained after stem vortex shedding was initiated.

4. Discussion

Entrainment of flocculent sediment in aquatic ecosystems is affected both by the properties of the floc, such as average size and density of aggregates, and also by the flow conditions in the vicinity of sediment source areas. Our field measurements of floc entrainment were generally consistent with results from a laboratory flume experiment that used Everglades floc (Larsen et al., 2009a). Floc entrainment increased substantially in the field (by a factor of 4) after hydraulic conditions changed to a stem vortex shedding regime,

which was consistent with bed shear stress exceeding a laboratory-determined critical value for entrainment of bed floc (Larsen et al., 2009a) in the field flume just as vortex shedding began. An important difference between the field and lab studies was that significant floc entrainment occurred on all velocity steps in the field flume, including under laminar flow conditions well below the critical shear stress for bed erosion. Epiphytic coatings on plants were the primary source of suspended floc during the lower steps of laminar flow. That source was augmented by bed erosion once stem vortex shedding was initiated. No plants with epiphyton were present in the laboratory flume (and some fine floc may have been lost during collection), which explains why floc entrainment in the laboratory was insignificant below a shear stress threshold for bed sediment entrainment. Mobilization of floc by detachment from epiphyton in the field flume explains why the amount of floc entrained in our field flume was more than an order of magnitude greater than predictions based on the laboratory flume experiment for similar hydraulic conditions calculated using Eq. [9] from Larsen et al. (2009a).

Finding mobilization of fine floc under conditions below a threshold for bed sediment entrainment is important for a number of reasons, not the least of which is that fine floc mobilized from epiphyton is more dense (Fig. 5) and more phosphorus-rich (Fig. 4c), and therefore contributes more to carbon and phosphorus transport per unit volume that is mobilized. Identifying epiphyton as the dominant source of suspended sediment between 1 and 3 cm s^{-1} is also important because of potential feedback interactions with flow. Our data show that epiphyton influences flow conditions due to the greater effective frontal areas and diameters of stems with epiphytic coatings. In the vicinity of our field flume the epiphytic coatings on spikerush species (*Eleocharis elongata* and *Eleocharis cellulosa*) increase the frontal areas by approximately 30% and the diameters by more than 50% (Table 3), which has substantial effects on vegetative drag and flow resistance (Nepf, 1999; Harvey et al., 2009).

4.1. Role of bioturbation and feeding of organisms in entraining floc at low velocities

Measurements of suspended sediment during ambient flow conditions in the flume were representative of conditions in the present-day water conservation areas in the Everglades (Noe et al., 2010). When bed shear stresses are not high enough to entrain bed sediment and also too low to mobilize significant amounts of floc from epiphyton, it is biological processes or weather related processes that entrain floc. For example, bioturbation of bed sediment by macroinvertebrates, shedding of floccules from epiphyton due to feeding activities of organisms, production of new organic particles (i.e., fecal material, detritus) in the water column, and resuspension after a hurricane appear to be the primary factors involved in the entrainment of floc at ambient flow (Noe et al., 2010; Larsen et al., 2009c). Our flume experiment has added to understanding of controls on entrainment by specifying under what conditions flocculent sediment on plant stems or on the sediment bed is mobilized by hydraulic forces.

Our data demonstrate that characteristics of suspended floc are highly variable with time at ambient flow. Before velocities were enhanced in the flume, the suspended floc in pumped water samples had an average size of approximately 53 μm and an average density of approximately 0.59 g cm^{-3} (Table 1). However, the second of the two individual samples during ambient flow had a relatively small average floc size (1.1 μm), whereas the first sample contained floccules much larger in size (108 μm) (Fig. 4). These results serve as a reminder that although coarse flocs (>100 μm) are not common in suspension during ambient flow, they do occur. During the first sample, the sub-samples from the middle and lower water column also differed substantially (Fig. 4) indicating a source of coarse floccules in the middle of the water column. Our interpretation is that the variability between samples during ambient flow resulted from intermittent shedding of coarse particles due to feeding activities, i.e. most likely grazing activities of *Gambusia holbrooki* (eastern mosquitofish) in the water column (Noe

Table 3
Mean frontal area, stem diameter, and vegetation biovolume in slough adjacent to experimental flume site.

	Vegetative frontal area, *a* (cm^{-1})				Stem diameter, *d* (cm)				Vegetation biovolume, *Vv/Vb*			
Vegetation with epiphyton removed	0–9.5 cm	9.5–19.5 cm	19.5–29.5 cm	Above water	0–9.5 cm	9.5–19.5 cm	19.5–29.5 cm	Above water	0–9.5 cm	9.5–19.5 cm	19.5–29.5 cm	Above water
Eleocharis elongata	4.1E−03	4.7E−03	4.8E−03	5.4E−04	0.07	0.07	0.07	0.06	9.7E−05	1.2E−04	1.6E−04	1.3E−05
Popup epipelon		9.3E−04	5.8E−03							2.4E−04	1.0E−03	
Eleocharis cellulosa	1.8E−03	1.3E−03	1.6E−03	8.8E−04	0.20	0.18	0.19	0.16	1.3E−04	7.9E−05	1.2E−04	6.0E−05
Nymphaea odorata[a]	2.0E−03	1.3E−03	9.1E−04		1.35	0.59	0.46	6.14	2.9E−04	1.1E−04	9.3E−05	
Panicum hemitomon			4.4E−05	2.2E−03			0.11	1.40			1.9E−06	1.5E−06
Paspalidium geminatum	9.7E−04	7.3E−04	7.8E−05		0.20	0.20	0.20		6.5E−05	5.2E−05	7.8E−06	
Utricularia purpurea			6.5E−04				0.04				5.9E−06	
Rhyncospora tracii				5.4E−05				0.07				2.5E−06
Nymphoides aquatica								1.65				
All species	8.9E−03	8.8E−03	1.4E−02	3.7E−03	0.24	0.12	0.11	0.24	5.8E−04	6.0E−04	1.4E−03	3.5E−04
	Vegetative frontal area, *a* (cm^{-1})				Stem diameter, *d* (cm)				Vegetation biovolume, *Vv/Vb*			
Vegetation including epiphyton	0–9.5 cm	9.5–19.5 cm	19.5–29.5 cm	Above water	0–9.5 cm	9.5–19.5 cm	19.5–29.5 cm	Above water	*e*	9.5–19.5 cm	19.5–29.5 cm	Above water
Eleocharis elongata	6.0E−03	1.2E−02	1.2E−02	5.5E−04	0.11	0.18	0.15	0.07	4.9E−04	1.7E−03	1.6E−03	2.7E−05
Popup epipelon		9.3E−04	5.8E−03							4.8E−04	2.0E−03	
Eleocharis cellulosa	2.3E−03	2.2E−03	2.1E−03	n/a	0.26	0.31	0.25	n/a	4.1E−04	5.3E−04	4.1E−04	1.2E−04
Nymphaea odorata	2.3E−03	1.7E−03	1.2E−03		0.22	0.27	0.24	n/a	6.9E−04	3.9E−04	2.6E−04	
Panicum hemitomon			9.1E−05	n/a			0.23	n/a			1.4E−05	2.9E−06
Paspalidium geminatum	1.4E−03	1.5E−03	1.0E−04		0.30	0.27	0.20		3.0E−04	4.5E−04	1.6E−05	
Utricularia purpurea			6.5E−04				0.04				1.2E−05	
Rhyncospora tracii				n/a				n/a				5.0E−06
Nymphoides aquatica								n/a				
All species	1.2E−02	1.8E−02	2.1E−02	3.7E−03	0.15	0.21	0.17	0.26	1.9E−03	3.6E−03	4.3E−03	6.9E−04

Data include live and dead macrophytes categorized by height increments, with each increment referenced by its height range in height above the floc surface. Vegetation data are also reported for live and dead material collected above the water surface at time of sampling. Blank cells indicate that the species was not present in that vertical increment. "n/a" indicates that no periphyton was present on the specimen.

[a] Floating *Nymphaea odorata* and *Nymphoides aquatica* leaves were not used in frontal area calculations.

et al., 2010; Larsen et al., 2009c). The LISST data collected every second during the ambient flow step support that interpretation. During the one-hour time period of ambient flow, the LISST detected coarse particles (>100 μm) in the water column only 28% of the time, and only 7% of the time were coarse particles present at volumetric concentrations greater than fine particles. These data confirm that coarse sediment entrainment is episodic from water column sources, at least during ambient flow. However, at higher flow velocities, coarse particles can be entrained from the plant canopy and sediment bed.

4.2. Multiple thresholds for floc entrainment in vegetated aquatic ecosystems

Floc entrainment occurred during all stages of our field experiment and increased immediately on both of the laminar flow steps when velocity was increased to 1.7 and 3.2 cm s^{-1}, respectively. Entrainment therefore occurred when bed shear stress was much too low (0.0008 and 0.004 Pa, respectively) for the flocculent sediment bed (critical entrainment threshold of 0.01 Pa) to be an important source. Thus, our interpretation is that during laminar flow the source of suspended floc is dominantly from epiphyton on plant stems, which suggests a considerably lower threshold for mobilization of floc from epiphyton compared to floc from the bed.

There are relatively few published studies of how flow velocity affects suspended sediment in shallow aquatic ecosystems with vegetation communities. Several previous studies have investigated removal of suspended sediment by settling on leaves of aquatic vegetation (Elliott, 2000) and interception of suspended particles onto stems. Leonard and Luther (1995) determined that interception of particles on stems of emergent macrophytes accounted for 10% of total sediment deposition in a brackish tidal marsh, whereas Stumpf (1983) found that interception of sediment by vegetation stems accounted for 50% of the removal of suspended particulates in a salt marsh. Palmer et al. (2004) examined interception experimentally in controlled conditions of laboratory flume and found that interception increases with the ratio of particle diameter relative to stem diameter and with the stem-based Reynolds number. Characteristics of stems such as stem roughness are also important. Palmer et al. (2004) found that stem roughness increased interception but acknowledged that more work is needed. Working in the Everglades, Saiers et al (2003) and Huang et al. (2008) found greater rates of sediment interception in spikerush (*Eleocharis elongata*)-dominated sloughs compared with sawgrass (*C. jamaicense*) dominated ridges. This finding may reflect the ten-times-smaller diameter of spikerush compared with sawgrass, which according to Palmer et al. (2004) should increase interception efficiency. Although not previously studied, entrainment of sediment from stem surfaces, (i.e., the reverse of interception on stems), is likely to be related to some of the same factors found to be important in interception, such as the stem-based Reynolds number for the flow, which influences shear forces near stems. Sediment adhesion to stems and shear forces involved in detachment of those particles has not to our knowledge been investigated in detail.

4.3. Relative contributions to floc entrainment from the bed and from vegetation stems

The flume experiment determined that there was a total of 46 g m^{-2} of potentially entrainable sediment, of which approximately half (26 g m^{-2}) was mobilized during the flow enhancement experiment (Tables 1 and 2). A comparison with measured inventories of epiphytic coatings and bed floc at the field site is revealing (Table 2) and indicates that floc in epiphyton is less abundant (66 g m^{-2}) than bed floc (330 g m^{-2}) and that both sources were present in quantities greater than what could potentially be entrained at velocities up to 6 cm s^{-1}.

Fine sediment (<100 μm) mobilized by detachment from epiphyton was the dominant contributor to entrainment during the initial laminar flow steps, whereas coarse sediment (>100 μm), including an unknown proportion contributed from the bed, contributed the larger proportion of the suspended sediment entrainment after vortex shedding flow conditions were initiated. It is important to acknowledge that we could not distinguish sediment mobilized from epiphyton from that mobilized from the bed once vortex shedding began because both reservoirs contain coarse and fine floc.

The relative importance of fine and coarse particles is evident after flow-weighting the fine and coarse textured concentration data

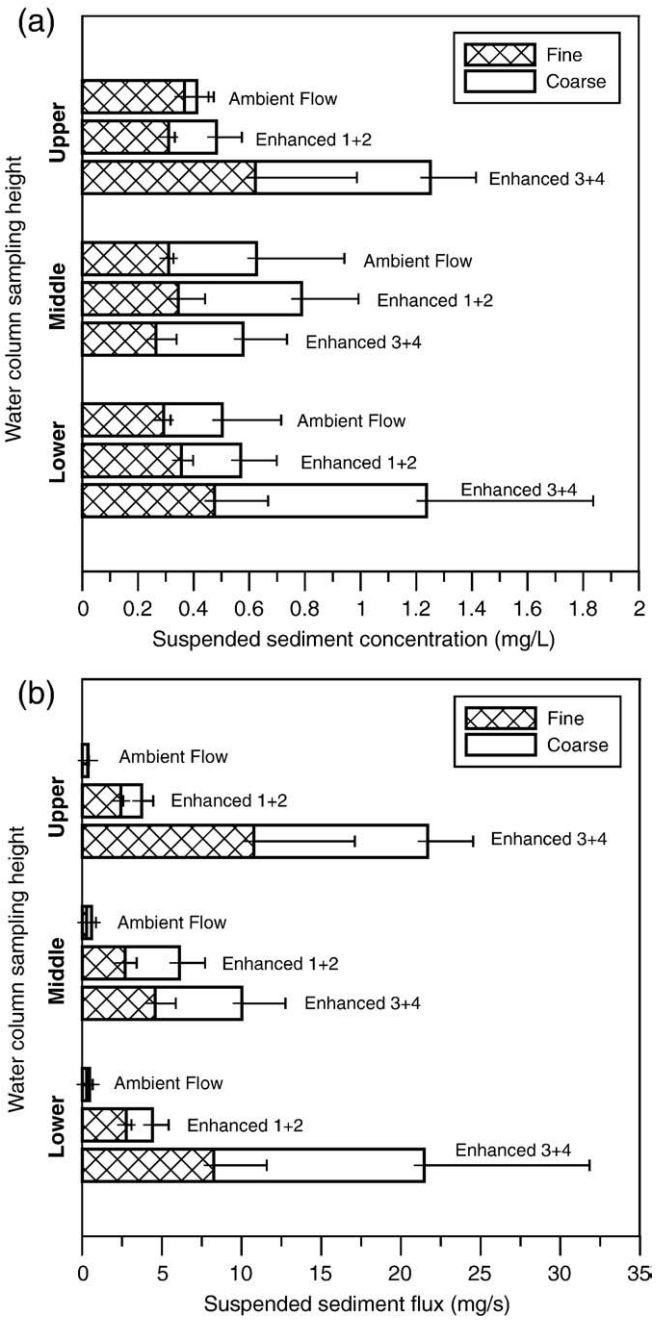

Fig. 8. Stacked bar graph of suspended sediment concentrations (a) and fluxes (b) showing contributions from fine (<100 μm) and coarse (>100 μm) aggregates during ambient flow without vortices downstream of stems, during enhanced flow steps 1 and 2 that were also laminar but with stable vortices, and during flow characterized by vortices shedding from alternate sides of stems during enhanced flow steps 3 and 4. Upper (24 cm above the bed), middle (16 cm), and lower (8 cm) sampling depths subdivided the 31.7 cm deep water column into four equal depth increments. Error bars represent standard errors of the mean for the peristaltic-pumped samples collected twice during ambient flow and four times for the combined enhanced flow steps.

(Fig. 8). Entrainment during the lower laminar flow steps (1 and 2) accounted for 21% of the total measured transport, with the larger proportion (57%) being accounted for by fine sediment. In contrast, 79% of the overall suspended sediment flux occurred during the higher flow steps with vortex shedding, with the smaller proportion (45%) being accounted for by fine sediment. The flux of sediment during ambient flow was insignificant relative to what occurred later and can be ignored in mass flux calculations.

The relative contributions of fine and coarse flocs to transport of suspended sediment varied over the experiment due to hydrodynamics and mobilization from different source areas (Fig. 8). The proportion of coarser floc generally increased with increasing velocity, both as an overall trend during the experiment and initially each time velocity was increased at the beginning of a new flow step. Coarse flocs were preferentially entrained on most velocity steps (Fig. 4b). Coarse flocs are therefore just as easily or possibly even more easily entrained than fine flocs at during a flow pulse of a given velocity. There are several caveats, however. At a given velocity the coarse reservoir of easily entrainable floc is quickly depleted and gives way to mobilization from a larger reservoir of relatively fine floc. Also, as already mentioned, the overall response over a range of flow velocities was an increasing mobilization of coarse flocs at the higher velocities.

4.4. Variation in phosphorus content in floccules of different size

Phosphorus associated with suspended sediment typically accounts for 13 to 57% of the total phosphorus concentration in the water column of the central Everglades (Noe et al., 2007; Noe et al., 2010). We found that the phosphorus density of floc (e.g. μmol P/mg) varies inversely with size (Fig. 4c). The negative relationship between size and phosphorus density of suspended sediment suggests that the fine suspended sediment comes primarily from a source with relatively high phosphorus density, whereas the coarse aggregates come from a source that is much poorer in phosphorus content. Finding that smaller flocs are more phosphorus-rich is consistent with previous research on fine floc in the Everglades indicating that very fine flocs are largely composed of aggregates of relatively labile primary particles including living bacteria and algal cells (Noe et al., 2007). In contrast, larger flocs are likely composed of older detrital organic matter with fewer attached colonies of bacteria and algae.

As a result of the coarsening of suspended floc at higher flows, the concentration of sediment-associated phosphorus in the water column did not increase as much with increasing velocity as did the overall flux of suspended sediment (Table 1). Thus, although suspended sediment flux increased by a factor of 47 during the experiment, the corresponding increase in phosphorus flux was only half of that (a factor of 23). In other words, higher flow velocities and the coarser floc that is transported cause the flux of sediment and organic carbon to increase much more than the flux of phosphorus.

An important additional finding is that the floc that was entrained in our experiment had a much higher concentration of phosphorus, regardless of size, than other potential bulk sources of suspended sediment (i.e., 0.16–0.57 μmol P/mg for suspended floc compared with approximately 0.008 μmol P/mg for bulk periphyton (Noe et al., 2001) and approximately 0.02 μmol/mg for bulk floc on the bed (Noe and Childers, 2007; Bruland et al., 2006)). The bulk population of periphyton and floc in the Everglades probably contain a large proportion of immobile material that is older and less labile on average. These results suggest that the floc that was mobilized by higher flows is probably more labile due to the considerably higher phosphorus content associated with active microbial and algal cells (Noe et al., 2007; Table 1), while the larger and less mobile flocs are relatively less enriched in phosphorus and are also less biogeochemically reactive.

4.5. Implications for phosphorus transport and redistribution in the everglades landscape

The overall importance of finding that mobile floc is enriched in phosphorus is its implication for downstream transport of phosphorus in this phosphorus limited ecosystem where contamination is a major problem. We found that pulsed flows mobilized floc from epiphyton on plants as well as from the bed, and that the size characteristics of entrained floc are a strong determinant of the phosphorus flux to downstream locations.

Also important was finding that transport of fine particles could be an important mechanism of redistributing phosphorus in the Everglades, which may contribute to processes that maintain the topographically and vegetatively diverse landscape. Our results suggest that redistribution of suspended material is highly limited at present-day ambient flows but begins to increase above flow velocities of 1.5 cm s^{-1}. These results are consistent with other recent findings. For example, Leonard et al. (2006) observed greater settlement of particles in sloughs than in ridges, and Neto et al. (2006) inferred using biomarkers that Everglades floc is generated *in situ* within slough or ridge. Noe et al. (2010) observed that the concentration of suspended sediment was low, did not differ between ridge and slough, and also did not correlate with water velocities below 1 cm s^{-1}. We observed that floc transport is enhanced substantially only after the threshold shear stress for bed sediment entrainment is exceeded (which occurred at a flow velocity above 3.5 cm s^{-1} in 32 cm of water in our experiment). Although flow velocities of that magnitude are rarely exceeded in the present, managed Everglades (Harvey et al., 2009), they may have occurred in the historic Everglades (Fennema et al., 1994). Our findings therefore support the hypothesis that reduction of flow velocities during the past century disrupted historic patterns of sediment redistribution that previously functioned as part of a complex physical–biological feedback system that shaped the parallel-drainage landscape (National Research Council, 2003; Larsen et al., 2007; Givnish et al., 2008).

4.6. Implications for increased understanding of physical–biological feedbacks in shallow aquatic ecosystems

Feedbacks between flow and vegetation are especially strong in shallow aquatic ecosystems and on floodplains where the substrate is organic soil formed by incomplete decomposition of emergent wetland vegetation. Larsen and Harvey (this issue) demonstrate through modeling the influence of feedbacks between flow and vegetation on hydrogeomorphology. The feedback cycle involves heterogeneities in flow through different vegetation communities that alter patterns of sediment redistribution and ultimately lead to self-organization of the landscape. Depending on a subtle balance between physical and biological factors, the topographic and vegetative patterns that are created can be highly linear and oriented either parallel or perpendicular to flow, or they can be more amorphous (Larsen and Harvey, this issue). A greater understanding of topographic and vegetative patterning in floodplains not only is important to protecting valuable ecosystem functions and services (e.g. biodiversity and habitat connectivity) but also has practical significance in the design of wetlands to enhance water treatment.

4.7. General implications for phosphorus and suspended sediment transport in vegetated flow systems

Quantifying the relative importance of fine and coarse suspended particle entrainment from two distinct sources in vegetated flow systems has general implications for how flow interacts with vegetation and organic particles to influence geomorphic and ecological processes in aquatic ecosystems. The fine particles entrained from epiphytic coatings on vegetation stems are higher in both bulk density and phosphorus content than coarse particles from the bed. Because

these fine particles from plant stems are much more easily entrained, they may play a proportionately greater role in ecological function of slowly flowing aquatic ecosystems. In addition to low-gradient floodplains like the Everglades there are wetlands constructed to treat wastewater where the fate of fine-particle associated phosphorus is also paramount (Kadlec and Knight 1996; Lightbody et al, 2007; Lightbody et al., 2008;Worman and Kronnas, 2005). Our novel observations of fine floc dynamics have implications for Everglades restoration and for the ecology of all vegetated aquatic ecosystems with organic sediment that experience laminar flows.

5. Summary

In situ field flume experiments in the Florida Everglades quantified entrainment of suspended sediment across 4 step increases in the laminar flow range. Each flow increase caused floc entrainment, even at very low velocities (e.g. 1.7 cm s^{-1}). Flow-vegetation interactions were characterized by creeping flow around stems under ambient conditions. At higher laminar flows, stable vortices formed downstream of stems. Relatively small sediment fluxes at flows in the lower laminar range increased abruptly (by a factor of four) after a bed shear stress threshold were surpassed at velocities above 3.2 cm s^{-1}, which coincided when vortices began shedding from alternate sides of stems.

Mobilization of floc from epiphytic coatings on plant stems and from the bed were the two primary sources of suspended sediment. During laminar flow with stable stem vortices, detachment of floc from epiphyton on plant stems was the dominant source and contributed 21% of the total measured entrainment during the experiment. The larger proportion of the entrainment (79%) occurred after vortex shedding by stems began and was contributed both by detachment from epiphyton and bed erosion. The experiment demonstrated that the critical shear stress determined for Everglades floc in a previous laboratory experiment (Larsen et al., 2009a) was a useful criterion for estimating when bed erosion of floc begins.

Within a single flow step the maximum entrainment and the size of suspended flocs tended to increase immediately after velocity increased and then decline with time as sediment sources became depleted. The entrained sediment coarsened over the experiment. Finer flocs less than 100 μm that were entrained from epiphyton made up the largest proportion of suspended sediment during laminar flow with stable vortices (Fig. 8). After stem vortex shedding began, it was coarser flocs greater than 100 μm that contributed the larger proportion. Floc size was important because it was negatively related to phosphorus content (i.e., the finer flocs were richer in phosphorus content compared with coarser flocs). As a result, as velocity increased, the magnitude of sediment and organic carbon fluxes grew faster than the phosphorus flux did due to a decreasing proportion of finer and more phosphorus-rich floccules being transported.

The floc entrained during the 4-hour experiment (26 g m^{-2}) was approximately half of the potentially entrainable floc reservoir (46 g m^{-2}) and was smaller than the measured inventory of bed floc (330 g m^{-2}) but similar in magnitude to the epiphyton inventory (66 g m^{-2}). The fine-grained and more phosphorus-rich floc was entrained first from epiphyton followed by bed erosion after stem vortex shedding began. Left behind was the relatively coarse and phosphorus-poor floc that made up the majority of the much larger and relatively immobile supply of bed floc that, regardless of size, has a phosphorus content (per gram) that is less than a tenth of the easily mobilizable floc. The floc bed stores a very large proportion of phosphorus in Everglades wetlands but only a small proportion is eventually buried as peat (Noe and Childers, 2007). Our study determined that high flow pulses are an effective means of transferring fine, phosphorus-rich flocs back to the water column by resuspension.

Everglades floc can be entrained at all velocities greater than or equal to 1.7 cm s^{-1} due to the ease of detachment of floc from epiphytic coatings on plant stems. Finding that the more mobile flocculent sediment in the Everglades is also the more phosphorus-rich and biologically active component of floc adds significantly to understanding of the phosphorus fate and transport in shallow aquatic ecosystems and also within constructed wetlands designed to remove phosphorus. However, many unknowns remain. For example, the proportion of floc supplied by bed erosion and epiphyton under stem vortex shedding flows could not be fully resolved by our study. Regarding the fate of the entrained floc, aggregation and disaggregation processes in the water column and the rate of settling can be estimated from other recent studies. However, field studies that estimate the rate at which suspended floc is removed by interception on plant stems are few (e.g. Saiers et al., 2003; Huang et al., 2008), and have typically used introduced single-particle tracers that are useful but not ideal analogues for naturally occurring aggregates. More investigations of plant interception of suspended sediment and shedding are needed, especially field investigations using the naturally derived aggregates of organic and mineral material that dominate suspended sediment in many shallow aquatic ecosystems.

Sediment entrainment from epiphyton has not been previously recognized as important in shallow vegetated aquatic ecosystems. However, it may contribute to transport and redistribution of organic carbon and phosphorus in ways that influence sediment accretion, topographic variability, water depth, and related ecosystem characteristics, including habitat diversity, habitat connectivity, and ability of ecosystems to adsorb and store excess nutrients and other contaminants.

Acknowledgements

The authors are grateful for the research support from the USGS Priority Ecosystems Science Program, the USGS National Research Program, NSF grant EAR-0732211, and the National Park Service Interagency Agreement F5284080024. We thank Leanna Westfall, Lars Soderqvist, and Craig Thompson for their assistance in field and laboratory work. Special thanks are due to Joe Wheaton, Robert Kadlec and two anonymous reviewers for the insightful comments that significantly improved the manuscript. Use of trade or product names is for descriptive purposes only and does not constitute endorsement by the USGS.

References

Aberle, J., Nikora, V., Walters, R., 2006. Data interpretation for in situ measurements of cohesive sediment erosion. J. Hydraul. Eng. 132 (6), 581. doi:10.1061/(ASCE)0733-9429.

Battin, T.J., Kaplan, L.A., Newbold, J.D., Hansen, C.M.E., 2003. Contributions of microbial biofilms to ecosystem processes in stream mesocosms. Nature 426, 439–442.

Bayley, P.B., 1991. The flood pulse advantage and the restoration of river-floodplain systems. Regul. Rivers Res. Manag. 6, 75–86. doi:10.1002/rrr.3450060203.

Bazante, J., Jacobi, G., Solo-Gabriele, H., Reed, D., Mitchell-Bruker, S., Childers, D., Leonard, L., Ross, M., 2006. Hydrologic measurements and implications for tree island formation within Everglades National Park. J. Hydrol. 329, 606–619.

Bendix, J., Hupp, C.R., 2000. Hydrological and geomorphological impacts on riparian plant communities. Hydrol. Proc. 14, 2977–2990.

Bernhardt, C.E., Willard, D.A., 2009. Response of the Everglades' ridge and slough landscape to late Holocene climate variability and 20th century water-management practices. Ecol. Appl 19 (7), 1723–1738.

Braskerud, B.C., 2001. The influence of vegetation on sedimentation and resuspension of soil particles in small constructed wetlands. J. Environ. Qual. 30, 1447–1457.

Browder, J.A., Gleason, P.J., Swift, D.R., 1994. Periphyton in the Everglades: spatial variation, environmental correlates, and ecological implications. In: Davis, S.M., Ogden, J.C. (Eds.), Everglades: the Ecosystem and its Restoration. St. Lucie Press, Delray Beach, pp. 379–418.

Bruland, G.L., Grunwald, S., Osborne, T.Z., Reddy, K.R., Newman, S., 2006. Spatial distribution of soil properties in Water Conservation Area 3 of the Everglades. Soil Sci. Soc. Am. J. 70, 1662–1676.

Cushing, C.E., Minshall, G.W., Newbold, J.D., 1993. Transport dynamics of fine particulate organic matter in two Idaho streams. Limnol. Oceanogr. 38 (6), 1101–1115.

Droppo, I.G., 2003. A new definition of suspended sediment: implications for the measurement and prediction of sediment transport. IAHS Publ. 283, 3–12.
Droppo, I.G., 2004. Structural controls on floc strength and transport. Can. J. Civil Eng. 31, 569–578.
Ellery, W.N., McCarthy, T.S., Smith, N.D., 2003. Vegetation, hydrology, and sedimentation patterns on the major distributary system of the Okavango Fan, Botswana. Wetlands 23, 357–375. doi:10.1672/11-20.
Elliott, A.H., 2000. Settling of fine sediment in a channel with emergent vegetation. J. Hydraul. Eng. 126, 560–577.
Fennema, R.J., Neidrauer, C.J., Johnson, R.A., MacVicar, T.K., Perkins, W.A., 1994. A computer model to simulate natural Everglades hydrology. In: Davis, S.M., Ogden, J. C. (Eds.), Everglades: the Ecosystem and its Restoration. St. Lucie Press, Boca Raton, FL, pp. 249–289.
Gaiser, E.E., Trexler, J.C., Richards, J.H., Childers, D.L., Lee, D., Edwards, A.L., Scinto, L.J., Jayachandran, K., Noe, G.B., Jones, R.D., 2005. Cascading ecological effects of low-level phosphorus enrichment in the Florida Everglades. J. Environ. Qual. 34, 717–723.
Galat, D.L., Fredrickson, L.H., Humburg, D.D., Bataille, K.J., Bodie, J.R., Dohrenwend, J., Gelwicks, G.T., Havel, J.E., Helmers, D.L., Hooker, J.B., Jones, J.R., Knowlton, M.F., Kubisiak, J., Mazourek, J., McColpin, A.C., Renken, R.B., Semlitsch, R.D., 1998. Flooding to restore connectivity of regulated, large-river wetlands. BioScience 48, 721–733.
Gerbersdorf, S.U., Jancke, T., Westrich, B., Paterson, D., 2008. Microbial stabilization of riverine sediments by extracellular polymeric substances. Geobiology 6, 57–69. doi:10.1111/j.1472-4669.2007.00120.x.
Gibbins, C., Vericat, D., Batalla, R.J., Gomez, C.M., 2007. Shaking and moving: low rates of sediment transport trigger mass drift of stream invertebrates. Can. J. Fish. Aquat. Sci. 64 (1), 1–5.
Givnish, T.J., Volin, J.C., Owen, V.D., Volin, V.C., Muss, J.D., Glaser, P.H., 2008. Vegetation differentiation in the patterned landscape of the central Everglades: importance of local and landscape drivers. Global Ecol. Biogeogr. 17, 384–402.
Harvey, J.W., Conklin, M.H., Koelsch, R.S., 2003. Predicting changes in hydrologic retention in an evolving semi-arid alluvial stream. Adv. Water Res. 26, 939–950. doi:10.1016/S0309-1708(03)00085-X.
Harvey, J.W., McCormick, P.V., 2009. Groundwater's significance to changing hydrology, water chemistry, and biological communities of a floodplain ecosystem, Everglades, South Florida, USA. Hydrogeol. J. 17, 185–201. doi:10.1007/s10040-008-0379-x.
Harvey, J.W., Schaffranek, R.W., Noe, G.B., Larsen, L.G., Nowacki, D., O'Connor, B.L., 2009. Hydroecological factors governing surface-water flow on a low-gradient floodplain. Water Resour. Res. 45, W03421. doi:10.1029/2008WR007129.
Huang, Y.H., Saiers, J.E., Harvey, J.W., Noe, G.B., Mylon, S., 2008. Advection, dispersion, and filtration of fine particles within emergent vegetation of the Florida Everglades. Wat, Resour, Res 44, W04408. doi:10.1029/2007WR006290.
Inoue, K., Nishimura, M., Nayak, B.B., Kogure, K., 2007. Separation of marine bacteria according to buoyant density by use of the density-dependent cell sorting method. Appl. Environ. Microbiol. 73 (4), 1049–1053. doi:10.1128/AEM.001158-06.
Junk, W.J., Bayley, P.B., Sparks, R.E., 1989. The flood pulse concept in river-floodplain systems. In: Dodge, D.P. (Ed.), Proceedings of the International Large River Symposium: Canadian Special Publications of Fisheries and Aquatic Sciences, 106, pp. 106–127.
Kadlec, R.H., Knight, R.L., 1996. Treatment Wetlands. CRC Press, Boca Raton, Florida. 893 pp.
Kremer, B., Kazmierczak, J., Stal, L.J., 2008. Calcium carbonate precipitation in cyanobacterial mats from sandy tidal flats of the North Sea. Geobilogy 6, 46–56. doi:10.1111/j.1472-4669.2007.00128.x.
Larsen, L.G., 2008. Hydroecological feedback processes governing self-organization of the Everglades ridge and slough landscape. Department of Civil, Environmental and Architectural Engineering, University of Colorado, Boulder, 320 pages.
Larsen, L. G., Harvey, J.W., this issue. Modeling of hydroecological feedbacks predicts distinct classes of wetland channel pattern and process that influence ecological function and restoration potential. *Geomorphology*.
Larsen, L.G., Harvey, J.W., Crimaldi, J.P., 2007. A delicate balance: ecohydrological feedbacks governing landscape morphology in a lotic peatland. Ecol. Monogr. 77 (4), 591–614.
Larsen, L.G., Harvey, J.W., Crimaldi, J.P., 2009a. Morphologic and transport properties of natural organic floc. Wat. Resour. Res. 45, W01410. doi:10.1029/2008WR006990.
Larsen, L.G., Harvey, J.W., Crimaldi, J.P., 2009b. Predicting bed shear stress and its role in sediment dynamics and restoration potential of the Everglades and other vegetated flow systems. Ecol. Eng. 35, 1773–1785. doi:10.1016/j.ecoleng.2009.09.002.
Larsen, L.G., Harvey, J.W., Noe, G.B., Crimaldi, J.P., 2009c. Predicting organic floc transport dynamics in shallow aquatic ecosystems: insights from the field, laboratory, and numerical modeling. Wat. Res. Res. 45, W01411. doi:10.1029/2008WR007221.
Leonard, L.A., Luther, M.E., 1995. Flow hydrodynamics in tidal marsh canopies. Limnol. Oceanogr. 40, 1474–1484.
Leonard, L.A., Reed, D.J., 2002. Hydrodynamics and sediment transport through tidal marsh canopies. J. Coastal Res. 36, 459–469.
Leonard, L., Croft, A., Childers, D., Mitchell-Bruker, S., Solo-Gabriele, H., Ross, M., 2006. Characteristics of surface-water flows in the ridge and slough landscape of Everglades National Park: implications for particulate transport. Hydrobiologia 569, 5–22.
Lick, W., Lick, J., Ziegler, K., 1992. Flocculation and its effect on the vertical transport of fine-grained sediments. Hydrobiologia 235 (236), 1–16.
Lightbody, A.F., Avener, M.E., Nepf, H.M., 2008. Observations of short-circuiting flow paths within a free-surface wetland in Augusta, Georgia, USA. Limnol. Oceanogr. 53, 1040–1053.
Lightbody, A.F., Nepf, H.M., Bays, J.S., 2007. Mixing in deep zones within constructed treatment wetlands. Ecol. Eng. 29, 209–220.
Logan, B.E., Wilkinson, D.B., 1990. Fractal geometry of marine snow and other biological aggregates. Limnol. Oceanogr. 35, 130–136.
Middleton, B.A., 2002. The flood pulse concept in wetland restoration. In: Middleton, B.A. (Ed.), Flood Pulsing in Wetlands: Restoring the Natural Hydrological Balance, pp. 1–10.
National Research Council, 2002. Riparian Areas: Functions and Strategies for Management. National Academies Press, Washington, DC. 444 pp.
National Research Council, 2003. Does Water Flow Influence Everglades Landscape Patterns?. National Academies Press, Washington, DC. 41 pp.
Nepf, H.M., 1999. Drag, turbulence, and diffusion in flow through emergent vegetation. Water Resour. Res. 35, 479–489.
Nepf, H.M., 2004. Vegetated flow dynamics. In: Fagherazzi, S., Marani, M., Blum, L.K. (Eds.), The Ecogeomorphology of Tidal Marshes. American Geophysical Union, Washington, DC, pp. 137–163.
Neto, R., Mead, R.N., Louda, W.J., Jaffe, R., 2006. Organic biogeochemistry of detrital flocculent material (floc) in a subtropical, coastal wetland. Biogeochemistry 77, 283–304.
Newbold, J.D., Thomas, S.A., Minshall, G.W., Cushing, C.E., Georgian, T., 2005. Deposition, benthic resistance, and resuspension of fine organic particles in a mountain stream. Limnol. Oceanogr. 50, 1571–1580.
Nezu, I., Onitsuka, K., 2001. Turbulent structures in partly vegetated open-channel flows with LDV and PIV measurements. J. Hydraulic Research 39 (No. 6), 629–642 IAHR.
Noe, G.B., Childers, D.L., 2007. Phosphorus budgets in Everglades wetland ecosystems: the effects of hydrology and nutrient enrichment. Wetlands Ecol. Manage. 15, 189–205. doi:10.1007/s11273-006-9023-5.
Noe, G.B., Childers, D.L., Jones, R.D., 2001. Phosphorus biogeochemistry and the impact of phosphorus enrichment: why is the Everglades so unique? Ecosystems 4, 603–624.
Noe, G.B., Harvey, J.W., Saiers, J., 2007. Characterization of suspended particles in Everglades wetlands. Limnol. Oceanogr. 52, 1166–1178.
Noe, G.B., Hupp, C.R., 2009. Retention of riverine sediment and nutrient loads by coastal plain floodplains. Ecosyst. 12, 728–746. doi:10.1007/s10021-009-9253-5.
Noe, G.B., Harvey, J., Schaffranek, R., Larsen, L., 2010. Controls of suspended sediment concentration, nutrient content, and transport in a subtropical wetland. Wetlands 30, 39–54. doi:10.1007/s13157-009-0002-5.
Odum, W.E., Odum, E.P., Odum, H.T., 1995. Nature's pulsing paradigm. Estuar. 18, 547–555.
Palmer, M.R., Nepf, H.M., Pettersson, T.J.R., Ackerman, J.D., 2004. Observations of particle capture on a cylindrical collector: implications for particle accumulation and removal in aquatic systems. Limnol. Oceanogr. 49, 76–85.
Poole, G.C., Daniel, S.J., Jones, K.L., Woessner, W.W., Berhnardt, E.S., Helton, A.M., Stanford, J. A., Boer, B.R., Beechie, T.J., 2008. Hydrologic spiralling: the role of multiple interactive flow paths in stream ecosystems. River Res. Applic. doi:10.1002/rra.1099.
Saiers, J.E., Harvey, J.W., Mylon, S.E., 2003. Surface-water transport of suspended matter through wetland vegetation of the Florida everglades. Geophys. Res. Lett. 30 (19), HLS 3-1–HLS 3-5.
Simon, M., Grossart, H.P., Schweitzer, B., Ploug, H., 2002. Microbial ecology of organic aggregates in aquatic ecosystems. Aquat. Microb. Ecol. 28, 175–211.
Stanturf, J.A., Schoenholtz, S.H., 1998. Soils and Landforms. In: Messina, M., Conner, W. (Eds.), Southern Forested Wetlands: Ecology and Management, pp. 123–148.
Sterling, M.C., Bonner, J.S., Ernest, A.N.S., Page, C.A., Autenrieth, R.L., 2005. Application of fractal flocculation and vertical transport model to aquatic sol-sediment systems. Water Res. 39, 1818–1830.
Stumpf, R.P., 1983. The process of sedimentation on the surface of a salt marsh. Estuarine, Coastal Shelf Sci. 17, 495–508.
Sumer, B.M., Fredsoe, J., 2006. Hydrodynamics around Cylindrical Structures (Revised Edition). World Scientific Publishing, Singapore. Advanced Series on Ocean Engineering.
Tabacchi, E., Lambs, L., Guilloy, H., Planty-Tabacchi, A., Muller, E., Décamps, H., 2000. Impacts of riparian vegetation on hydrological processes, *Hydrol. Process.*, 14, 2959–2976. doi:10.1002/1099-1085(200011/12)14:16/17<2959::AID-HYP129>3.0.CO;2-B0.
Tockner, K., Lorang, M.S., Stanford, J.A., 2010. River flood plains are model ecosystems to test general hydrogeomorphic and ecological concepts. River Res. Applic. doi:10.1002/rra.1328.
Tockner, K., Malard, F., Ward, J.V., 2000. An extension of the flood pulse concept. Hydrol. Process. 14, 2861–2883. doi:10.1002/1099-1085(200011/12)14:16/17.
Walling, D.E., Moorhead, P.W., 1989. The particle size characteristics of fluvial suspended sediment: an overview. Hydrobiologia 176/177, 125–149.
Willard, D.A., Cronin, T.M., 2007. Paleoecology and ecosystem restoration: case studies from Chesapeake Bay and the Florida Everglades. Front. Ecol. Environ. 5 (9), 491–498.
Winterwerp, J.C., vanKesteren, W.G.M., 2004. Introduction to the physics of cohesive sediment in the marine environment. Developments in Sedimentology, 56. Elsevier, Amsterdam. 466 pp.
Wotton, R.S., 2007. Do benthic biologists pay enough attention to aggregates formed in the water column of streams and rivers? J. N. Am. Benthol. Soc. 26, 1–11.
Worman, A., Kronnas, V., 2005. Effect of pond shape and vegetation heterogeneity on flow and treatment performance of constructed wetlands. J. Hydrol. 301, 123–128.
Zweig, C.L., Kitchens, W.M., 2009. Multi-state succession in wetlands: a novel use of state and transition models. Ecology 90 (7), 1900–1909.